Combination of Multi-modal Imaging and Neurophysiology to Improve Targeting Accuracy and Outcome in Deep Brain Stimulation for Movement Disorders

By Paul Moran

Supervisory team:

Dr Maria Braoudaki
Mr Nik Haliasos
Dr Mahmoud Iravani

'submitted to the University of Hertfordshire in partial fulfilment of the requirement of the degree of Masters by Research'.

May 2021

i)   <u>Abstract</u>

A study was conducted to observe the positioning of two sets of electrodes in fourteen patients with Parkinson's disease (PD). The purpose was to potentially optimise electrode positioning and parameters with the goal of possibly benefiting patient outcome. Boston scientific electrodes were the multi-directional electrodes (also known as directional) and Medtronic 3389 were the conventional electrodes, each set had been previously surgically inserted into PD patients with pre- and post-operative imaging data available. The corresponding data was input into Lead DBS software to identify the hypothetical electrode position in silico. A target point within the most central point of the motor region of subthalamic nucleus (mSTN) was selected with the corresponding distance measured from the active contact of each patient electrode. The mean electrode distance observed from the target point to active contact in all patients was (right) 6.52 millimeter (mm) (SD=2.75, SE=0.83) and (left) 5.91mm (SD=2.83, SE= 0.82). The mean voltage was (right) 1.36V (SD=0.74, SE=0.2) and (left) 1.64V (SD=0.89, SE=0.25). No UPDRS data was available due to limited access to databases as a result of travel restrictions imposed rendering the study qualitative in nature. It was not possible to determine what electrode would be more successful to alleviate symptoms given the small cohort in each arm of the study. It was also not possible to determine if Diffusion tensor imaging (DTI) could be used as a tool in aiding in the reduction of volume of tissue activated outside of the desired area again due to low numbers of DTI data sets available. This study was able to optimize electrode parameters within Lead-DBS; however, this could not be replicated in a clinical setting as further research would be required to validate the results of this study. No firm conclusion can be drawn between the advantages and disadvantages of each type of electrode.

ii)   **Table of Contents**

iii)　　List of Images

iv)　　List of Tables

v)　　Appendices

1. Introduction

1.1 Brain Structure

The brain, which is the processing unit of the human body possesses a number of different neurons developing numerous connections, in order to deduce a signal relay from one sub structure to another. Located in the cranium of mammals the brain is divided into three broad sections, the forebrain, midbrain and hind brain (Table 1). The forebrain is further split into two sections, the telencephalon and the diencephalon. The telencephalon also known as the cerebrum has four main lobes; the frontal, temporal, parietal and occipital and is divided into two hemispheres by longitudinal fissure. The left hemisphere controls the right-hand side of the body, whereas the right hemisphere controls the left-hand side of the body with the two sections being connected by the corpus callosum; a bundle of nerve fibres relaying signals between them. The midbrain or mesencephalon is part of the brain stem located at the posterior section of the brain. The hind brain is divided into two sections; the metencephalon containing the cerebellum and the myelencephalon containing the medulla oblongata (Grinblat & Lipinski, 2019).

Table 1: Structures within the brain. The table shows the different structures and substructures of the brain.

Location	Main Structure	Lobes	Sub structures
Forebrain	Telencephalon	Frontal Lobe Temporal Lobe Parietal Lobe Occipital Lobe	Basal Ganglia Hippocampus Olfactory bulb
	Diencephalon	N/A	Thalamus Hypothalamus Subthalamus Epithalamus
Midbrain	Mesencephalon	N/A	Substantia nigra Red Nucleus
Hindbrain	Metencephalon	N/A	Cerebellum Pons
	Myelencephalon	N/A	Medulla oblongata

The basal ganglia (Figure 1), a subsection responsible for functions including voluntary motor control, habit forming behaviour and emotion is located deep within the brain, predominantly in the telencephalon located within the fore brain. The basal ganglia contain smaller substructures in different areas such as the subthalamic nucleus (STN) located in the diencephalon and the substantia nigra (SN) located in the midbrain (Lanciego, Luquin, & Obeso, 2012).
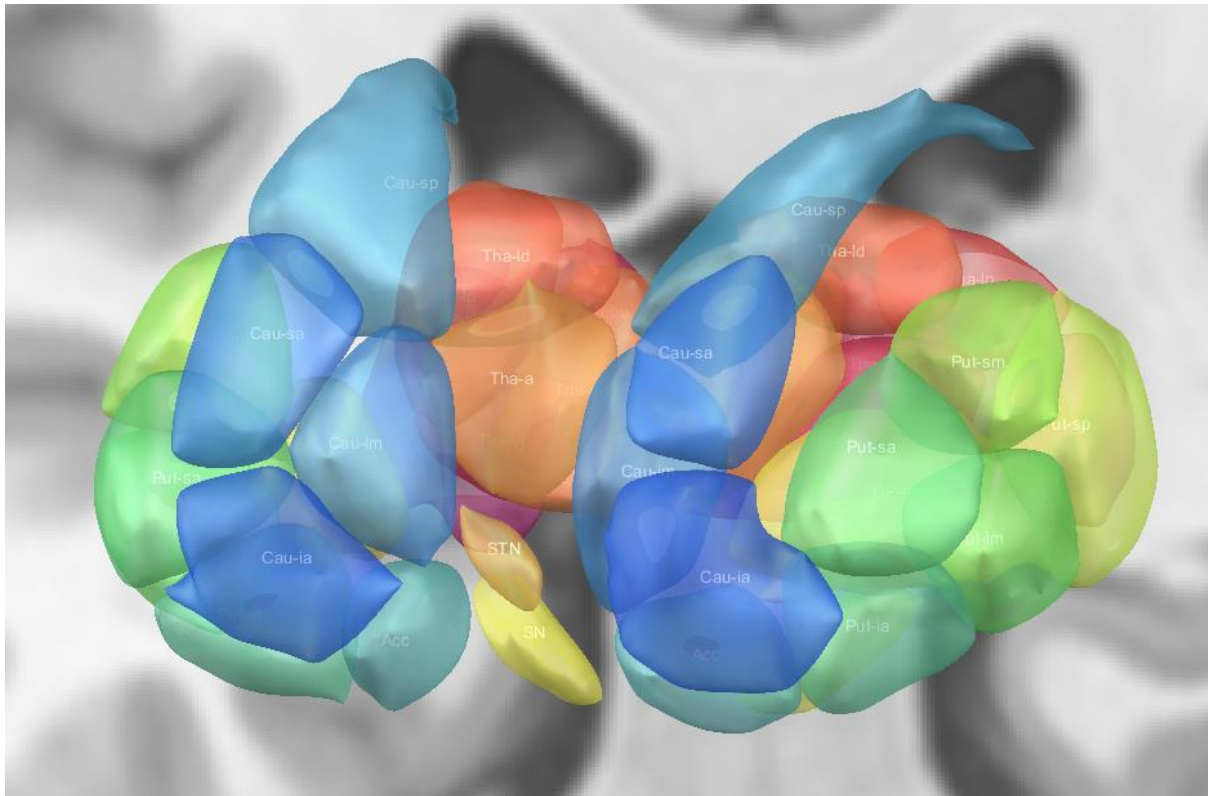
Figure 1: Anatomy of the basal ganglia. The Figure shows the sub structures located within the basal ganglia. The cortex sends signals to the Putamen and Caudate nucleus both of which make up the striatum. The striatum sends signals to the GPe, GPi and the SN. The STN is a downstream target of the GPe and upstream target of the GPi and SN in the indirect pathway (Image adapted from Lead DBS, 2021).

There are two pathways (figure 2) activated within the basal ganglia that work in conjunction to perform smooth movement namely the direct and indirect pathway. The direct pathway promotes movement, whereas the indirect decreases movement. A signal transduction pathway is activated in the supplementary motor area (SMA) within the cortex, releasing excitatory glutaminergic neurotransmitters that are received by the striatum. This triggers the release of gamma aminobutyric acid (GABA), an amino acid that operates as a neurotransmitter. GABA inhibits the neuronal projections of the internus globus pallidus (GPi) and SN, at which time dopamine produced within the SNr is projected onto the D1 receptors of the striatum causing further GABA induced inhibition of GPi and SN. As a result, the thalamus receives a decreased signal from the GPi, causing an excitatory signal back to the SMA promoting movement, for decreased movement the indirect pathway is activated. The SMA projects an excitatory signal to the striatum that inhibits the external globus pallidus (GPe), this inhibits the signal received by the STN resulting in an excitatory signal projecting onto the GPi and SN. Dopamine release from the SNc binds to D2 receptors on the striatum via the nigrostriatal pathway resulting in increased inhibition of the thalamus decreasing activation within the SMA (Freeze, et al., 2013; Eagel, et al., 2011).
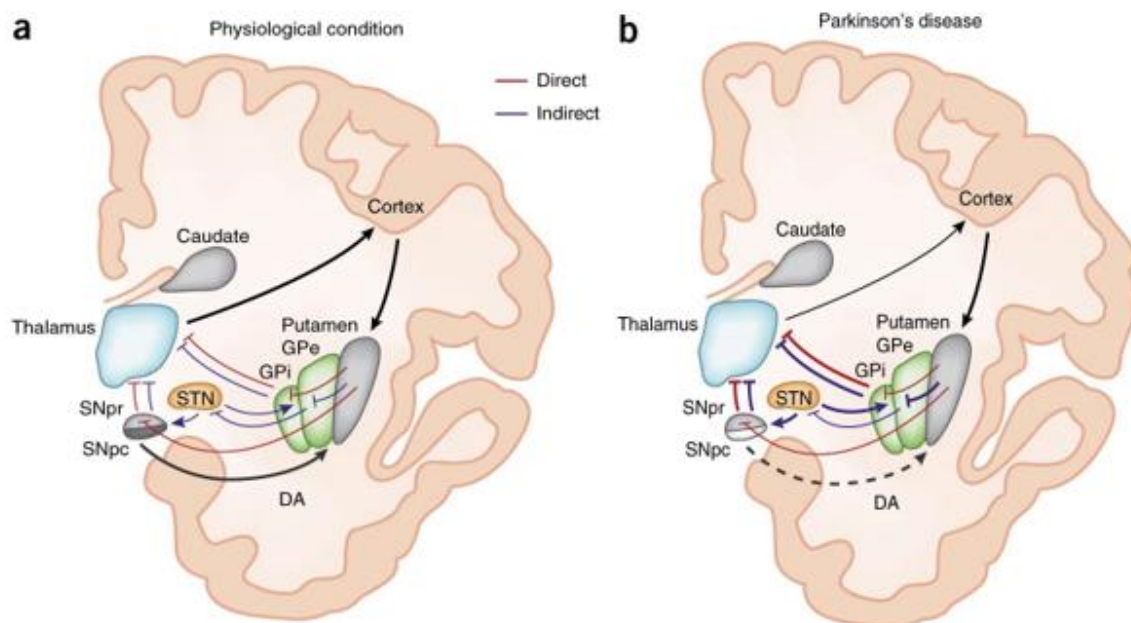
Figure 2: Direct and indirect pathway within the basal ganglia. The Figure shows the direct and indirect pathway within the basal ganglia. A is the neuronal pathway under regular conditions whereas B is the parkinsonian state. In B neuronal projects from the SNc (shown as substantia nigra pars compacta) have been significantly reduced resulting in decreased stimulation of the putamen (Calabresi et al., 2014).

1.2 Parkinson's Disease

Parkinson's disease (PD) is a neurological condition largely affecting movement resulting from the loss of dopaminergic neurones in the substantia nigra. This causes the loss of dopaminergic nerve terminals in the caudate and putamen nucleus. Consequently, causing an imbalance between the activity of the direct and indirect striatal output pathways. Currently, there is no cure for PD however, symptoms can be mitigated by use of dopaminergic medicine and surgery. The lack of dopamine in the SN can result in tremors, involutory shaking, rigidity and bradykinesia (DeMaagd & Phillip, 2015). The ventrolateral region of the SN is predominantly where the neural loss occurs, paired with the proliferation and growth of astrocytes, further identifying one of the main hallmarks of the disease (Gibb, 1992). Observations state motor defects are present upon destruction of 50% of dopaminergic neurones in the SN (Cheng, Ulane, & Burke, 2010; Ross, et al., 2004) with other studies identifying 80% loss (Masato et al., 2019). Lower levels of dopamine result in the decreased stimulation through the nigrostriatal pathway to the striatum further amplifying the inhibitory signals received by the GPe leading to decreased and disordered movement (Qiu et al., 2016). The imbalance of neurotransmitter levels, due to decreased volume of dopamine results in symptoms observed in patients with PD. A number of genes are known to be involved in PD development, such as *Parkin* and *LRRK2* (leucine-rich repeat kinase 2), the complete mechanism of upstream and downstream regulation remains unclear.

The formation of protein aggregates is a significant hallmark of PD, with implicated genes such as *SNCA* (alpha synuclein*)* playing a key role in Lewy body formation.

1.3 Dopamine, Mechanism, and Receptors

The tyrosine hydroxylase (*TH*) gene produces the TH enzyme that catalyses the conversion of the non-essential amino acid, tyrosine to levodopa (Figure 3). In the final step, dopamine is produced from levodopa by catabolism from the enzyme dopa-decarboxylase. Dopamine is stored in vesicles located on neuronal axons, upon arrival of an action potential the permeability of the neuronal cell membrane is increased allowing dopamine to enter into the synaptic cleft, a space between neurons where it will be up taken by the receiving cell or degraded upon re-entry by the sending cell (Daubner, Le, & Wang, 2010).
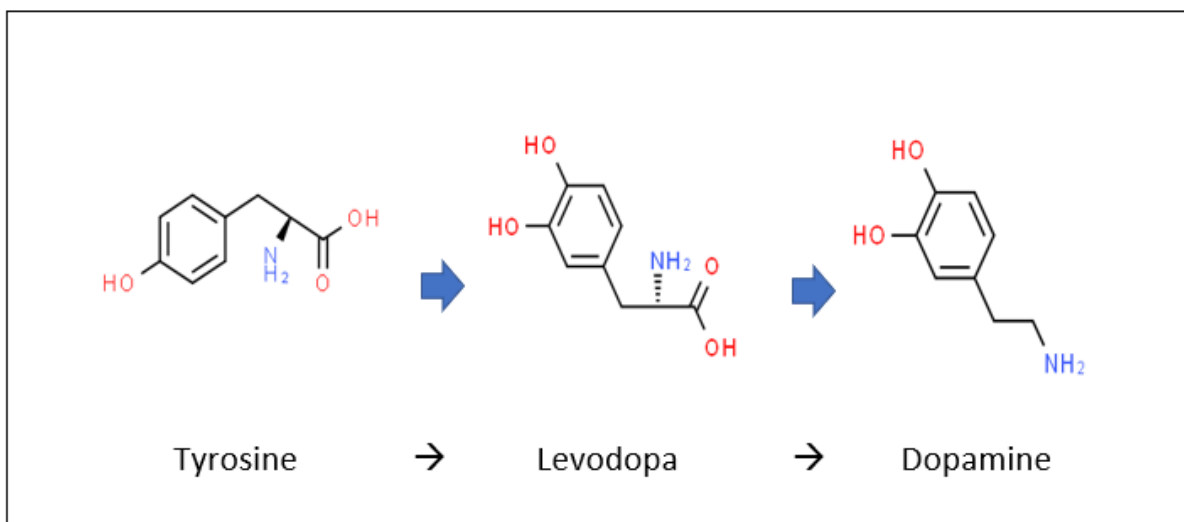
Figure 3: Dopamine conversion. The conversion of tyrosine into dopamine is shown. Initially the amino acid tyrosine is converted to the dopamine precursor levodopa. The cleavage of the carboxylic acid group on levodopa successfully activates the molecule by turning it into dopamine (Adapted from: Uniprot, 2020).

Dopamine stimulation contributes to the increase or decrease of movement depending on what receptor it is bound to; this situation is more complicated as stimulation of both D1 and D2 receptors can result in increased movement. Stimulation of D1 receptors activate direct striatal output resulting in increased movement. Stimulation of D2 receptors inhibits indirect pathway activation which inhibits movement meaning disinhibition of the indirect pathway will cause movement.

 Initially, the SN projects onto the caudate and the putamen, both of which make up the striatum. Glutamate produces an excitatory response within the striatum, whereas dopamine produces an inhibitory response. Dopamine is secreted from two different sections of the SN. Firstly, dopamine produced by the SNc amplifies the direct pathway by way of binding to D1 class receptors located

within the striatum. Secondly, D2 class receptors within the striatum are targeted by SNr dopamine release in the indirect pathway. Dopamine binds G protein coupled receptors (GPCR), specifically subreceptor D_1 and D_5 from the D1 like receptor family and D_2, D_3 and D_4 from the D2 like receptor family. Dopamine in the synaptic cleft binds to GPCRs on the adjacent target cell, however, excess dopamine will re-enter the previous neuronal cell and the remaining dopamine will be metabolised by two specific types of enzymes located within a different type of non-neuronal cell called a glial cell. The enzymes are called monoamine oxidase type B (MAOB); the anti-depressant and PD target and also catechol-0-methyltransferase (COMT) another PD drug target (Tritsch & Sabatini, 2012).

Dopamine binding of different subreceptor in the D1 and D2 like receptor family will initiate a signal transduction pathway and determine the appropriate cellular response (Figure 4). Different $G\alpha_s$ and $G\alpha_{olf}$ family subunits that are part of the trimeric GTP binding protein complex become activated upon ligand dependent binding of D1 like receptors resulting in a GDP to GTP molecule displacement. The GTP/Alpha complex selectively binds to the adenylyl cyclase. ATP is converted to cyclic AMP by adenylyl cyclase which is used to activate protein kinase A (PKA) by dissociating PKA from the membrane bound PKA inhibitors. PKA further takes a phosphate group from ATP (converting to ADP) to regulate different cellular components (Neve, Seamans & Trantham-Davidson 2004).
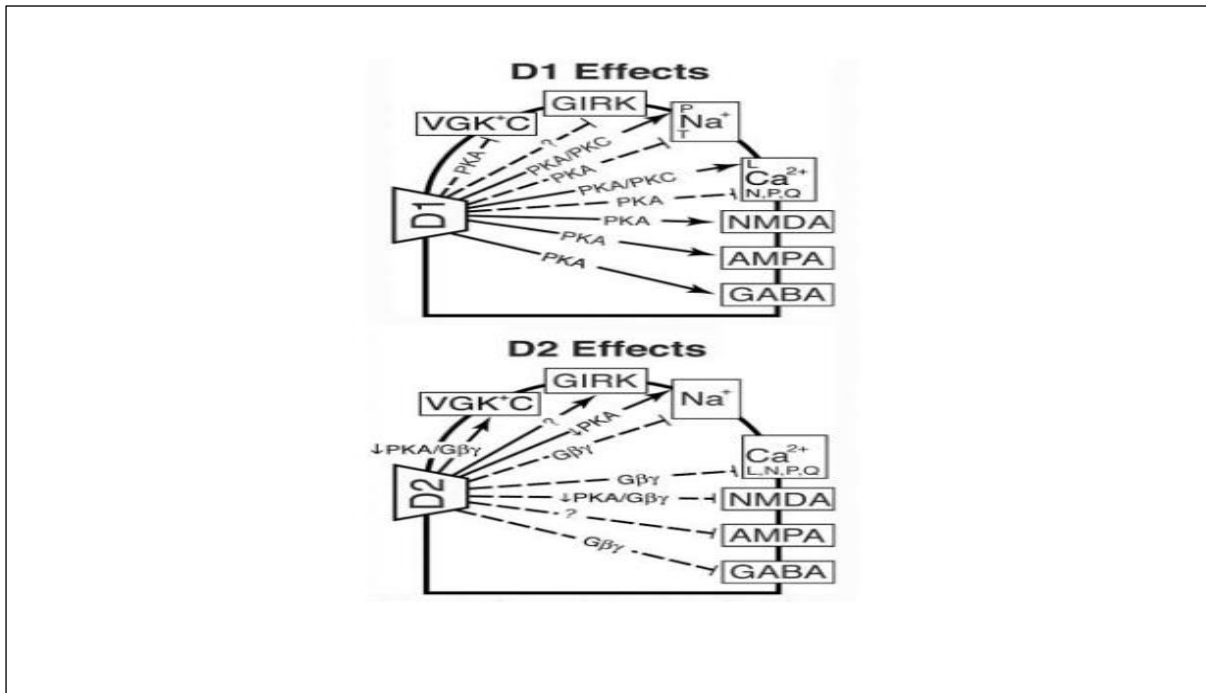
Figure 4: Effects of D1 and D2 like receptor binding under normal function. D1 like receptor binding predominantly activates protein kinase A, which upregulates many different cell receptors. D2 like receptors (continued) activate protein kinase A as well as the beta/gamma subunits of the now dissociated trimeric GTP binding protein. D1 and D2 like receptor family inactivation due to lack of dopamine has a considerable knock-on effect to many different cellular pathways responsible for normal function of the cell (Adapted from Neve, Seamans & Trantham-Davidson 2004).

1.4 Molecular Mechanism of Key Genes

Parkinson's disease is thought to have an underline genetic cause, which may be either inherited or environmental. A plethora of genes have been identified to play a significant role in PD manifestation with some better documented such as the *LRRK2*, *Pink1* and *Parkin* genes (Klein & Westenberger, 2012). The resulting misfolded proteins accumilate to form protein aggregates. The combination of SNCA, hyperphosphorylated tau (p-tau) and amyloid beta can be observed in PD patients that have a secondary neurologcal condition such as dementia. Misfolded protein aggregates vastly contribute to cognitive decline through mechinisms such as oxidative stress and mitochondrial damage. It is suggested that the agregates may form a membrane pore in patients with PD allowing for the aformentioned degenration mechanisms (Maiti, Manna, & Dunbar, 2017).

1.4.1 *Pink1 and Parkin*

Specific gene mutations leading to the production of deficient proteins can contribute to the disease. An example of this is *Pink1* and *Parkin* mutations. On normal mitochondrial function, Pink1 is taken from the cytosol and transported inside the mitochondria. In disease state, the electrochemical gradient of H^+ used to drive ATP synthesis is lost. Pink1 is no longer able to enter the mitochondria, instead residing on the surface subsequently recruiting parkin, a ubiquitin ligase protein that tags the mitochondria and the cell for destruction. The normal and deficient function can be seen in Figure 5. Early onset PD usually occurs in individuals with *Pink1* and *Parkin* gene mutations before the age of 45. However, there is no fixed age for individuals with these mutations. There have been documented cases of children as young as seven years old that present with PD (Lücking, et al., 2000; Jin & Youle, 2012).
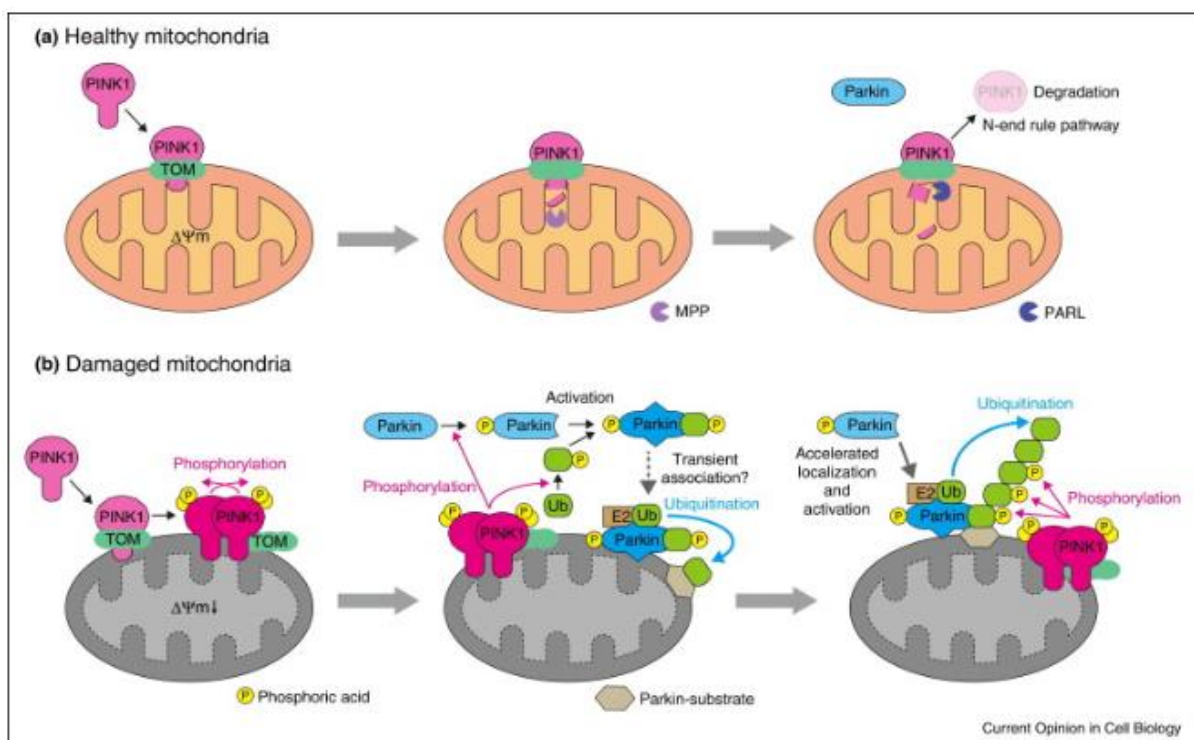
Figure 5: Healthy and damaged mitochondria (page 10)**.** The Figure shows the mechanism of *Pink1* and *Parkin*. In normal conditions, Pink1 partially crosses the mitochondria membrane releasing a substrate that gets processed. The result of natural function is Parkin remains inactive in the cytosol. When Pink1 cannot cross the mitochondrial boundary, it self-dimerises and phosphorylates parkin and ubiquitin. The phosphorylated parkin resides on the mitochondrial surface and gets poly ubiquitinated until destruction is complete (Adapted from Eiyama & Okamoto, 2015).

Parkin also plays a role in the formation of Lewy bodies, a pathological hallmark of PD and dementia. Lewy bodies are made up from SNCA protein, ubiquitin and neurofilaments. The ubiquitin-proteasome system (UPS) regulates various cell functions including the viability of the cell. SNCA is a key part of the UPS complex and any mutations in the protein will contribute towards the formation of aggregates, namely Lewy bodies (Betarbet, Sherer, & Greenamyre, 2005).

1.4.2 *LRRK2* gene

The *LRRK2* gene, which is located on chromosome twelve has been identified in the heredity and sporadic acquisition of PD. It has been suspected that the G2019S missense gene mutation may be involved in 3% of Parkinsonian cases; however, this number may be higher. As the mutation is prominent in disease state, LRRK2 drug inhibitors are currently in the clinical stages to nullify the effect of the mutation. The gene codes for a kinase protein that phosphorylates other proteins specifically Ras-associated binding (RAB) proteins; G proteins that are a member of the RAS superfamily. The excessive phosphorylation of RAB by the LRRK2 protein decreases the activity of the RAB proteins and contributes to parkinsonian disease state. The exact mechanism remains to be elucidated with an area of current PD research focusing on this gene and its downstream mechanisms. It has also been shown that the LRRK2 protein hyper-phosphorylates the signalling adapter protein P62; however, this depends on an operative C-terminus ubiquitin domain (Kalogeropulou et al., 2018).

It has been suggested that LRRK2 may have a dual role in pathogenesis of PD. Firstly, LRRK2 may contribute to Lewy body formation by increased stimulation of SNCA transcription resulting in increased protein aggregate formation. SNCA is known to stimulate microglial activation with the end result being neuroinflammation and cell death. The second mechanism of upregulated LRRK2 activity is believed to be over phosphorylation of specific downstream targets involved in neuronal apoptotic pathway namely the mitogen-activated protein kinase pathway. Both pathways that result from increased levels of activated LRRK2 result in neuronal cell death (Rui, Ni, Li, Gao, & Chen, 2018)

1.5 Epidemiology

At any one time, there are 1-2% of the population living with PD, with 1% of the population over 60 years-old developing the disease (Tysnes & Storstein, 2017). A meta-analysis study of mortality due to PD and prevalence from 1990 to 2016 showed an alarming trend. In 1990, there were 2.5 million people living with PD globally. In 2016, 6.1 million people were diagnosed with the disease worldwide

(Figure 6). In just over 25 years the number of people with the disease has doubled largely due to the population living for a longer time span (Dorsey et al., 2018.1).
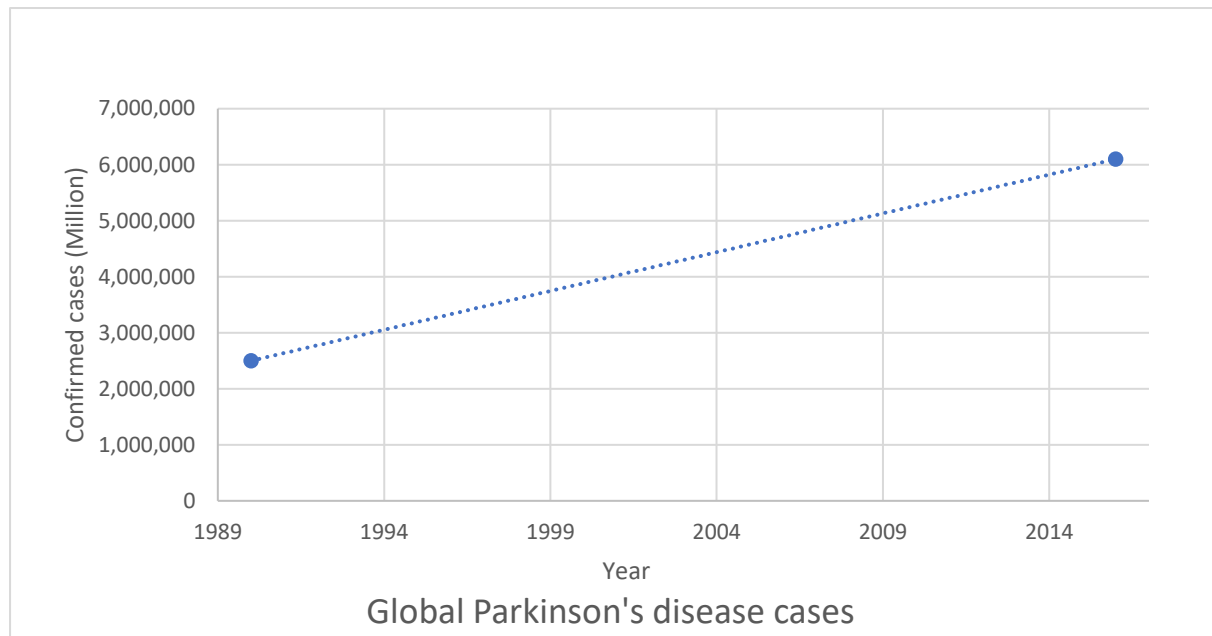
Figure 6: Confirmed cases of Parkinson's disease worldwide. The graph shows the number of confirmed cases of Parkinson's disease globally. In 1990 represented by point A, there were 2.5 million new cases. In 2016 there were a reported 6.1 million new cases (adapted from global, regional, and national burden of neurological disorders, 1990-2016: a systematic analysis for the global burden of disease study. Dorsey et al,. 2018.2)

Parkinson's disease caused 211,296 deaths and 3.2 million adjusted life years in 2016, suggestive of potential years lost when compared to average life expectancy. The ratio of male to female of age standardised prevalence were similar in 1990 and 2016 showing a level of consistency of the disease susceptibility (Dorsey, et al., 2018.3). One study conducted over a 38-year period identified patients with PD were twice as likely to succumb to its effects as a secondary factor with many of those diagnosed passing away from pneumonia and cardiovascular disease (Pinter et al., 2015).

Parkinson's disease is the second most common neurological disease after Alzheimer's disease (AD) and the second most common movement disorder after essential tremor (ET). Tremor is a symptom of PD but presents differently to ET. Parkinsonian tremor predominantly occurs in a rest state, whereas ET occurs during movement, however this is not true for every case (Thenganatt & Louis, 2012).

Parkinson's disease is observed in all ethnic groups; however, location contributes to prevalence of disease. There are more confirmed cases in developed countries, as people are living longer into old age due to better health care and general living conditions. People with direct family members that suffer with PD are 4-fold more likely to develop PD when compared to people without a family link

(Alves, et al., 2008). Familial linked PD usually occurs before 50 years of age and has a tendency to be a more aggressive when compared to idiopathic PD with research linking genes such as *LRRK2*, *Pink1*, *Parkin* and *DJ-1* to a higher risk of developing PD (Redensek, Trost & Dolzan, 2017)

1.6 Diagnosis

There are various methods to diagnose PD. Early detection sometimes appears to be more difficult with a number of cases misdiagnosed for other common neurological diseases, due to the overlap in observable non-motor symptoms. Only once patients have succumbed to the disease can Lewy bodies be observed in the midbrain by an autopsy. Abnormalities in the SN can be detected by diffusion tensor imaging (DTI) magnetic resonance imaging (MRI), in which the loss of water flow is observed indicating neuronal destruction in the specific area again pointing toward disease state (Brooks, 2012). Positron emission tomography (PET) with fluorodopa and single photon emission computed tomography (SPECT) are both used in diagnosis. Upon radionuclide decay, gamma radiation is produced and dissipated into surrounding tissue that can be directly measured by PET and SPECT (Lu & Yuan, 2015). There are physical signs, such as tremor and bradykinesia, which indicate a Parkinsonian state (Rand, Stelmach, & Bloedel, 2000); however, on occasion further evidence is required for a conclusive diagnosis. Tremor, the most common symptom falls into two broad classifications; the first is resting tremor that exhibits a frequency of 4-6Hz and the second is an action tremor. Action tremors have a range of subtypes including postural tremor, which has a frequency of 8-12Hz. Tremor is a significant hallmark of PD, however, not all patients present with this symptom and as a result require a more in-depth analysis to confirm responsiveness to levodopa. Frequencies in the range of 8-12Hz generate from oscillations in the central nervous system, with frequencies of 20-25Hz generated as feedback oscillations from mechanical reflexes (Vaillancourt & Newell, 2000). The patient can experience non-motor symptoms all relating to the disease including hyposmia or loss of smell, constipation or issues related to Rapid eye movement (REM) sleep, also known as REM sleep behaviour disorder. Lastly, depression and anxiety can also be present (Reichmann, 2017). Once PD has been confirmed the unified Parkinson Disease Rating Scale (UPDRS) is used to determine the severity of disease. There are four segments used within the UPDRS scale; behavioural and mood, activities of daily living (ADL), motor examination, complication of therapy. Additional two extra scales may be used called Hoehn and Yahr staging, and Schwab and England ADL (Movement disorder society task force, 2003).

1.7 Prognosis

The prognosis for PD tends to be unfavourable with worsening symptoms and cognitive decline increasing as a result of progressive cell loss as the disease progresses. Studies highlighted the relationship between body mass index (BMI) and prognosis for PD. It was shown that the majority of individuals who suffered with the disease often lose weight and have a lower BMI. In male subjects, a lower BMI is shown to be more detrimental, whereas a higher BMI in females produces a more favourable prognosis linked to longer survival (Park, et al., 2018).

A study conducted in 2005 identified specific risk factors that impacted favourable prognosis. In general, patients with PD were more likely to develop dementia if they carried the apolipoprotein E gene (APOE) ε2 allele. The mortality rate was a median of 9.1 years from first diagnosis of PD, regardless of gender or genetic predisposition. Patients who developed dementia as a result of their parkinsonian condition had an increased chance of mortality (Lau, et al 2005).

1.8 Drug Treatment

In recent years, a variety of different drugs have been tested to determine their effectiveness in relieving parkinsonian symptoms. Several drugs such as levodopa have demonstrated a better long-term outcome for PD patients, but often produce undesired side effects after an extended period of time such as levodopa induced dyskinesia (Bezaed, Brotchie, & Gross, 2001). The production of levodopa has also limited the demand for new drugs as levodopa successfully mimics the role of dopamine and our current knowledge identifies dopamine as a key driver in PD. Difficulty resides in the initial stages, as there are challenges in replicating the natural mechanism of PD in animal models. Currently, 6-hydroxydopamine model rats and 1-methyl-4-phenyl-1,2,3,6-tetrahydropyridine monkeys are being used for research, as the compounds result in an artificial PD state for the animal (Tieu, 2011).

1.8.1 Levodopa

Levodopa is administered alongside carbidopa or benserazide (Rinne & Molsa, 1979), and has long been considered the gold standard of drug treatment for PD (Poewe et al., 2010). Levodopa produced from tyrosine, the precursor to dopamine holds a similar chemical structure to dopamine, but with an extra carboxyl group. Levodopa can be administered orally in tablet form or with carbidopa as a liquid suspension known as duodopa gel. The surgically inserted peg-j tube is terminated in the proximal

jejunum of the small intestine allowing for the drugs to be administered directly into the body (Montgomery et al., 2016).

For a greater amount of levodopa to successfully reach the brain, carbidopa is normally administered simultaneously. Carbidopa is a decarboxylase inhibitor that stops the cleavage of the carboxyl group of levodopa keeping it in its inactive form in the periphery. This halts levodopa conversion before it reaches the brain however, carbidopa is unable to cross the blood brain barrier resulting in levodopa crossing unaccompanied (Ovallath & Sulthana, 2017). Continual administration can result in sickness, dizziness, and sleep issues and in some instances, levodopa induced dyskinesia in > 40% of cases (Alhskog & Muenster, 2001). Defined as an involuntary movement with the two most common types of dyskinesia being dystonia and chorea is a direct result of the continued on and off stimulation from levodopa (Vasta, et al., 2017). Dyskinesia falls into three categories, peak dose dyskinesia, where levodopa is at its highest level in plasma also the most common type. The second is off peak dystonia usually occurring in the morning and resulting in involuntary leg movement. The third is diphasic dyskinesia that produces involuntary leg movement that occurs approximately 15 minutes after levodopa administration or soon before the effects of the medication start to fade (Pandy & Srivanitchapoom, 2017).

1.8.2 Dopamine Agonists

Dopamine receptor agonists resemble the chemical structure of dopamine which bind and activate the dopamine associated receptor families D1 and D2 like receptors; however, there are not any clinically useful D1 agonists currently in use. Dopamine receptor agonist fall into two main categories; ergoline and non-ergoline (Gerlach, et al., 2003.1). Ergolines, which are derived from ergot alkaloids include and pergolide and bromocriptine. Pergolide acts on both D1 and D2 receptors whereas bromocriptine binds to the subreceptor D_2 located in the striatum. The D_2 receptor is grouped with inhibitory G-proteins decreasing the action of adenylyl cyclase resulting in the cAMP signal transduction pathway being disrupted. The second set of dopamine agonists include pramipexole and ropinirole. The mechanism of non-ergoline class of dopamine agonists is not well understood. Ropinirole binds to the D2 like receptors D_2 and D_3. The D_3 receptors are clustered in the limbic area of the brain and upon activation produce a neuroprotective effect. Again, the D_2 activation results in inhibition of adenylyl cyclase with the receptors believed to be located in the caudate – putamen area of the striatum (Gerlach et al., 2003.2).

1.8.3 Monoamine Oxidase Type B Inhibitors

Monoamine oxidase type B (MAO-B) inhibitors are another common class of drugs used to treat PD. They may be given in conjunction with levodopa and carbidopa to increase the efficacy of levodopa (Krishna, Ali, & Moustafa, 2014). MAO-B, a naturally occurring enzyme breaks down excess dopamine from the synaptic cleft that re-enters the original neuronal cell. The mechanism of MAO-B inhibitors is by binding and deactivating MAO-B in turn halting the degradation of excess dopamine produced as a result of levodopa (Finberg & Rabey, 2016).

1.8.4 Anticholinergic Drugs

The first class of drugs used to treat PD were identified to be competitive agonists of various subtypes of muscarinic receptors known collectively as anticholinergic drugs. The drugs given orally are most successful when targeting the resting tremor. It has been stated that the inhibition of acetylcholine in the basal ganglia partially restores the balance between dopamine and acetylcholine resulting in an improved state in early-stage PD (Brocks, 1999). The treatment has shown to have limitations as levodopa normally takes over as main treatment in the later stages (Brocks, 1999).

1.8.5 Surgical Treatment

Surgical intervention for PD is predominantly a later stage treatment for patients that experience side effects from once successful drugs, where upon all non-invasive measures have been tried and tested and are deemed no longer adequate. Surgery may also be recommended for patients that have early onset PD as symptoms may be aggressive and prove difficult to treat, with dyskinesia being more prevalent (Merola, et al., 2012).

In the case of drug resistance PD, patients given this option are predominantly in the advanced stages of the disease, whereby severe variations of hypermobility and immobility occur in a short time frame, thus severely affecting the patient's quality of life. The NHS provides a set of criteria which must be met by prospective deep brain stimulation (DBS) surgical patients to undergo the surgery. Firstly, patients with an established diagnosis must be capable of enduring surgery under general anaesthetic, with prior evidence showing no signs of coagulopathy or sepsis. Additional requirements state a minimum life expectancy of 5 years, a L-dopa response greater than 40% after a set "medication off" period and a disabling off state that lasts a minimum of 30% of a 24-hour time frame (NHS Commissioning Board, 2013).

A preoperative MRI or CT scan is conducted to view the surgical targets within the basal ganglia for electrode placement. The motor region located at the dorsal lateral region of the STN is the predominant target as it can potentially alleviate both symptoms of rigidity and tremor, the GPi may also be targeted to address motor symptoms. One study identified targeting the STN identified a reduction of medication whereas GPi targeting was shown to improve PDQ-39 score (Peng et al., 2018). Patients may be asked the dominant symptom, in the case of tremor dominance patients may be given the option to have the electrodes (Figure 7) placed within the posterior subthalamic area (PSA), a zone outside of the STN specifically targeting the Dento-Rubro-thalamic (DTR) tract. DTR targeting has been shown to combat tremor, although patients may still experience bradykinesia. During the preoperative scan stage, PD patients will undergo general anaesthetic, with the purpose of minimising artifact development in the produced images, due to movement. Blood thinning drugs such as aspirin, warfarin and ibuprofen are prohibited before surgery, with specific PD medication also stopped. The purpose is to observe the success of the treatment as patients will be in an off-stage resulting in more pronounced symptoms beforehand. Coordinates of the STN are gathered from preoperative images providing a target point for electrode placement. Upon completion, the local anaesthetic is injected into different points around the skull, for a stereotactic frame to be attached to the patient's cranium. This allows for the neurosurgeon to map the coordinates gathered from preoperative imaging. Patients are woken up for surgery and will remain awake throughout the duration of the surgery, however, may be given a sedative to calm movement. An approximate 3mm hole is bored into the skull with the electrode wires placed within the desired target location (NHS OUH, 2017). Micro electrode recording (MER) is a method used for optimum electrode localisation, as the microelectrodes are lowered through the cerebrum action potentials are recorded from neuronal firing, which provides data from voltage changes in relation to time, this is visualised though neuronal firing pattern of spikes. Each area the electrode passes through has a different rate of firing and signifies what area and position the electrode currently resides. Upon final placement of the electrode, the neurosurgeon will use a number of different stimulation parameters to identify the optimum stimuli to alleviate symptoms. The final stage of the surgery is the placement of an implantable pulse generator (IPG), usually implanted in the chest. The IPG can be programmed to produce different stimulation parameters to lead to the optimum outcome for the patient. Changes in voltage/amperes will be conducted by a neurologist in a follow up programming session (NHS OUH, 2017).
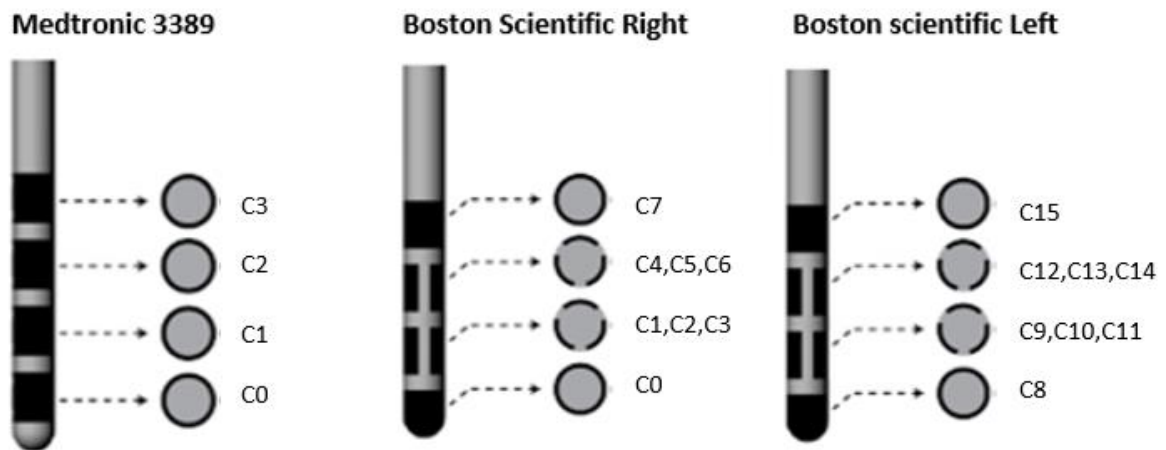
Figure 7: Multi-directional and conventional electrodes. The Medtronic 3389 (left) electrodes and the Boston Scientific directed (right) electrodes. The Medtronic electrodes contain four contacts whereas the Boston Scientific electrodes have a total of 16, 8 on each side, with the second and third band on each contact split into 3 different contacts enabling the electrode to become multi-directional (Solpsema, et al., 2018).

1.9 Hypothesis

It is hypothesized that the multi-directional Boston scientific electrodes will show a greater capacity when compared to the conventional method of non-directional Medtronic 3389 electrodes through analysis in Lead DBS. Medtronic 3389 electrodes can only operate in ring mode with non-directional targeting, whereas the Boston scientific vercise electrodes possess the ability to stimulate in a set direction. The use of multi-directional electrodes may improve PD patient outcome given the ability to target specific directions and lower the undesired volume of tissue (VTA) activated outside of the target area.

1.9.1 Aim

The aim of the research is to optimise DBS electrode parameters for patients who suffer with idiopathic PD using lead DBS. Patient data will be placed into computational software to analyse electrode positions, with the purpose of identifying an optimum location. Secondly, individual patient contacts used with resulting VTA will be observed to potentially identify a closer target point with the view to a hypothetical reduction of electrical stimulation.

1.9.2 Objectives

1. Parkinson's disease patients will have pre- and post-operative MRI data placed into Lead DBS for analysis in order to visualise electrode placement.

2. Patient data from post-surgical follow up programming sessions will be used to replicate the real time stimulation currently used for each patient. The VTA will be observed in relation to the mSTN of each patient. An additional target point will be selected in a central location of mSTN to observe a hypothetical potential reduction in stimulation using the mathematical formula observing the distance of two points in 3-dimensional space.

1.9.3 Research Questions

1) Which type of electrode is more effective to alleviate symptoms?

2) Can DTI tractography be used to lower volume of tissue activated outside of desired area and potentially identify activated neuronal tracts?

3) Is the use of multi-directional electrodes quicker and easier than the widely used conventional method?

4) Can electrode stimulation be optimised?

5) Using Lead DBS can a more specific point within the motor region of the subthalamic nucleus be identified as a target for DBS?

2. Methods

2.1 Patients

A total of 14 patients with idiopathic PD who underwent STN bilateral electrode placement surgery at Queens hospital were selected for DBS electrode position analysis though Lead DBS. The patient age range was 52-72. Seven patients (VG, GL, MB, JS, AW, KN, MS) had multi-directional Boston scientific electrodes and seven (TM, BD, GB, NH, JSc, GW, BP) had the conventional Medtronic 3389 electrodes. Patient data from post-surgical follow up programming sessions was gathered from the NHS database with all imaging data anonymised for patient confidentiality.

Prior to any research, a letter agreement between Barking, Havering and Redbridge University Hospitals, Queens's Hospital (BHRUT) and University of Hertfordshire was signed on 28th November 2019. Informed written consent was given by all the patients prior to enrolment in the study. The present study was conducted with the ethical approval of The Vice Chair of the Health, Science, Engineering and Technology ECDA, University of Hertfordshire (UH protocol number LMS/PGR/NHS/02946). Also, HRA and Health & Care Research Wales (CHCRW) approval has been given for this study (IRAS project ID: 273497, Sponsors No.; 129171, Protocol no. 1.0, Rec Ref 20/LO/0221). Each patient was assigned a code and all data sets were analysed anonymously.

2.2 Surgical Procedure

Patients were required to have a pre-operative MRI scan on the day of surgery allowing for electrode position selection. Patients were under general anaesthetic for imaging to minimise MRI artifact development. A stereotactic frame was placed on the skull of each patient allowing for trajectory coordinates to be implemented. Micro electrode recording was used to manoeuvre electrodes into the correct position through various structures in the brain. Patients were awoken for stimulation and testing of the electrode parameters with the aim of identifying any side effects. Upon satisfactory completion burr hole covers were placed over the incision holes with leads connected to an IPG placed within the chest area of patients. A comprehensive programming session was completed approximately 4 weeks after surgery.

2.3 Lead DBS

Patients had pre- and post-operative MRI data comprising of T1 and T2 weighted images placed into the Lead DBS software (Figure 8). The initial MRI data was in DICOM format were converted to the NIftI file format using dcm2niix. Anat_t2 was linearly co-registered to anat_t1 using SPM12. Postop_tra was linearly co-registered to anat_t1 using SPM12. Postop_sag was linearly co-registered to anat_t1 using SPM12 (Friston 2011; http://www.fil.ion.ucl.ac.uk/spm/software/) or Pre- (and post-) operative acquisitions were spatially normalized into MNI_ICBM_2009b_NLIN_ASYM space (Fonov 2011) based on preoperative acquisition(s) (anat_t2.nii, anat_t1.nii) using the SyN registration approach as implemented in Advanced Normalization Tools (Avants 2008; http://stnava.github.io/ANTs/). Nonlinear deformation into template space was achieved in five stages: After two linear (rigid followed by affine) steps, a nonlinear (whole brain) SyN-registration stage was followed by two nonlinear SyN-registrations that consecutively focused on the area of interest as defined by subcortical masks in Schoenecker 2008.

DBS-Electrodes were manually localised based on post-operative acquisitions using a tool specifically designed for this task (as implemented in Lead-DBS software; Horn & Kuehn 2005; SCR_002915; https://www.lead-dbs.org). Coordinates of specific contacts were gathered using the manual electrode localisation tool.

Atlas used for 3D visualization: DISTAL Minimal Atlas (Ewert 2017). Manual coordinates of activated electrode contacts were recorded. Once images were rendered 3D, two points were selected in the motor region of the visualised STN (figure 9B). The coordinates were placed centrally at either side of the mSTN with the central point identified using a mathematical formula (figure 9A). As the left STN was parallel to the right STN the opposing coordinates were used. The distance was measured from each activated contact to the target point within the left and right STN.
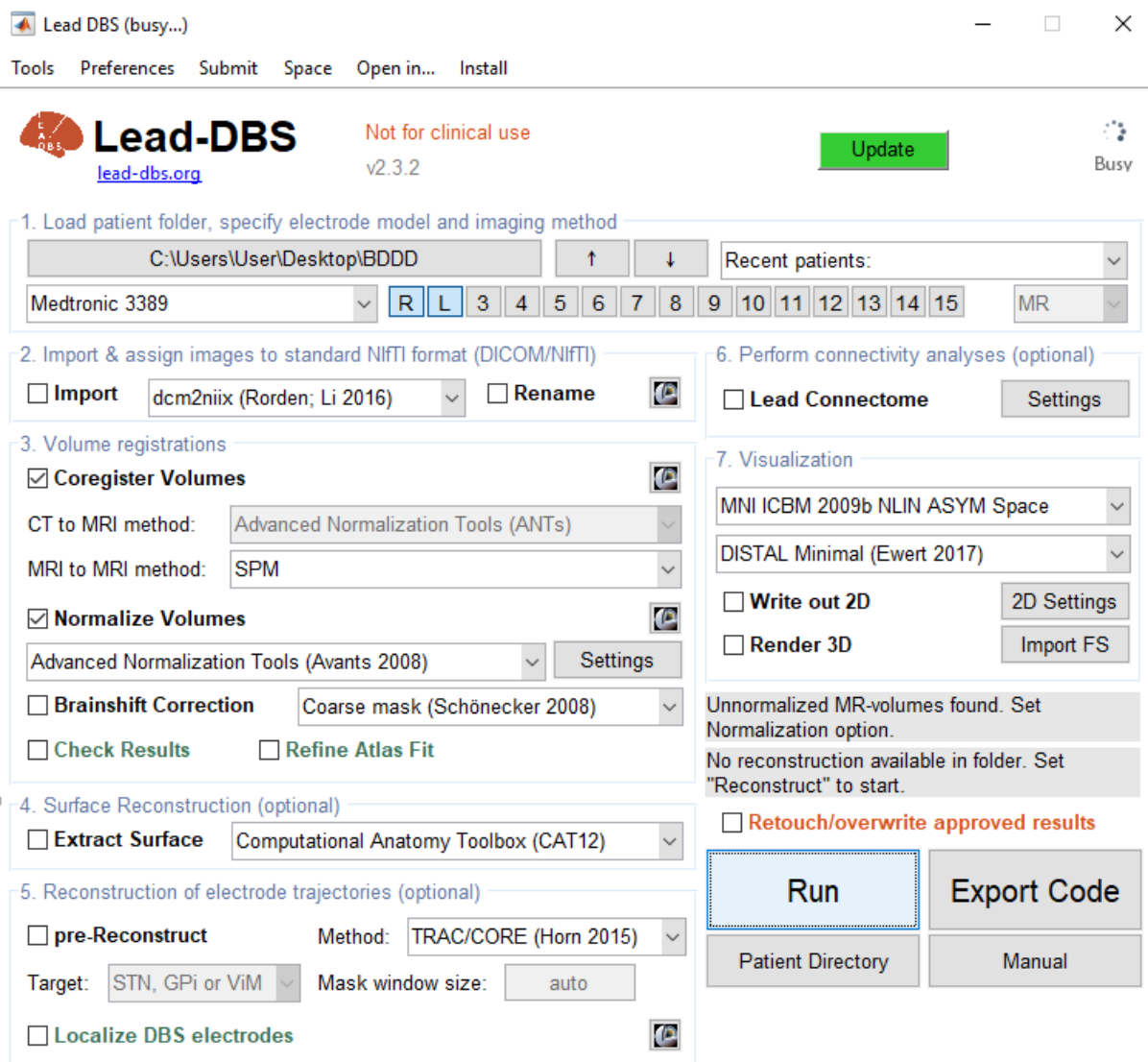
Figure 8: Lead DBS user interface. The figure shows all the steps required to successfully convert pre- and post-operative images to a visualised image identifying electrode placement.

Once images were rendered 3D with final electrode positions, visualisation of volume of tissue activated used the Simbio/fieldtrip (Horn 2017) stimulation parameters.

The contact in closest proximity to the selected point within the STN was identified. A reduction in stimulation was calculated using the patient data and both sets of coordinates, identifying the potential reduction that would produce the same result.

For DTI data sets, connectome results AICHA (Joliot 2015) were used to visualise neuronal tracts. A whole-brain fibre-set was estimated based using the Generalized q-sampling imaging (GQI) approach (Yeh 2010) as implemented in DSI-Studio (http://dsi-studio.labsolver.org). GQI is a model-free method that calculates the orientational distribution of the density of diffusing water. Fibres were sampled

within a white-matter mask that was estimated using the anatomical acquisition by applying the Unified Segmentation approach (Ashburner 2005) as implemented in SPM12. This mask was linearly co-registered to the b0-weighted series. The whole-brain fibre set was normalized into standard-stereotactic space following the approach described in (Horn 2014, Horn 2016) as implemented in Lead-DBS software (Horn 2015; www.lead-dbs.org).

```
2        % distance
3 -      x1=input('enter value of x1:\n');
4 -      x2=input('enter value of x2:\n');
5 -      y1=input('enter value of y1:\n');
6 -      y2=input('enter value of y2:\n');
7 -      z1=input('enter value of z1:\n');
8 -      z2=input('enter value of z2:\n');
9 -      distance =sqrt((x1-x2)^2+(y1-y2)^2+(z1-z2)^2)
```

X 12.7322
Y -15.2339
Z -5.905

X 13.6302
Y -13.7917
Z -8.00262
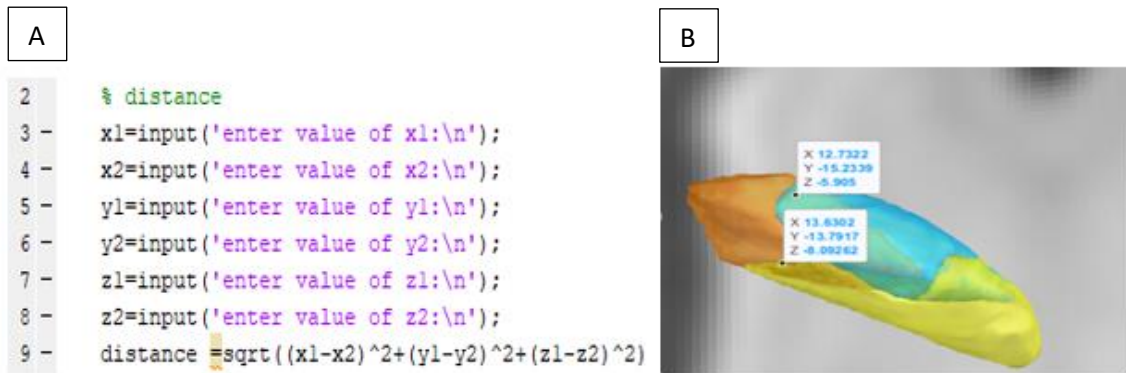
Figure 9A and B: Matlab formula and STN coordinates. Matlab script (left) to identify distance between two points in three-dimensional space and (right) coordinates selected on each side of the STN. The central point of the two coordinates was calculated using the Matlab formula.

3. Results

Fourteen patients with idiopathic PD were analysed after DBS electrode implantation. Seven by the standard Medtronic 3389 electrodes and seven were using Boston scientific vercise multi-directional electrodes. All patients had MRI data anonymously placed into the Lead DBS software to visualise final electrode placement (see appendices A - M). The corresponding electrode stimulation and distance of each electrode to the dorsal lateral region of the STN can be observed in Table 2.

**Table 2: Coordinates of target point in mSTN.**

Right STN coordinates (mm)	Left STN coordinates (mm)
X = 13.1812	X = 13.1812
Y = -14.5128	Y = -14.5128
Z = -6.9981	Z = -6.9981

3.1 Overall Patient Data

The mean electrode distance observed in all patients from the target point selected within the mSTN to each active patient contact was (right) 6.52mm (SD=2.75, SE=0.83) and (left) 5.91mm (SD=2.83, SE= 0.82). The mean voltage was (right) 1.36V (SD=0.74, SE=0.2) and (left) 1.64V (SD=0.89, SE=0.25). There was no correlation between voltage and distance, JSc (left) was observed as having a stimulation of 1.5V to alleviate symptoms with an observable distance of 0.7mm from active contact to mSTN, whereas BP (left) was 10.90mm and a stimulus of 1.4V. Patient MB (right) distance observed was 2.77mm with a 1.5V stimulation, BP (right) active contact was 13.33mm from target point with a 1.4V stimulation to alleviate symptoms highlighting no observable relationship. All electrodes bar GL (right) were placed into ring mode. In total, five electrodes (two right, three left) from twelve viable subjects were in the optimum location. Overall, 19 electrodes could have a hypothetical voltage reduction as a closer contact to the target point was observed.

3.2 Coordinate Selection

Each patient had the coordinates of the active contact used to measure the distance from the target point coordinates within the left and right STN of each patient. The right electrode (Figure 10) was manually adjusted within Lead DBS.
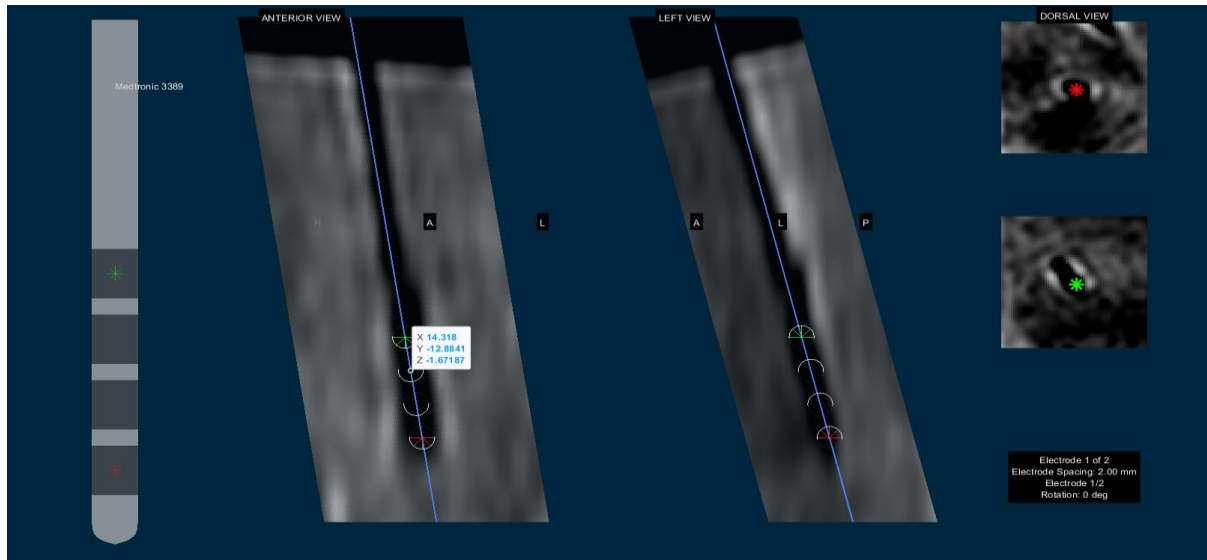
Figure 10: Manual electrode placement of right-side electrode. Patient NH, identifying coordinates of selected contact. The electrode is identified by the artifact produced by the electrode in postoperative scan. The dorsal view (top right) shows the trajectory from above whereas the anterior and left view identify the downward trajectory.

The artifact produced from the electrode during post-operative MRI scan was used to place the electrode in the correct position. The left electrode (Figure 11) was placed in the same manner.
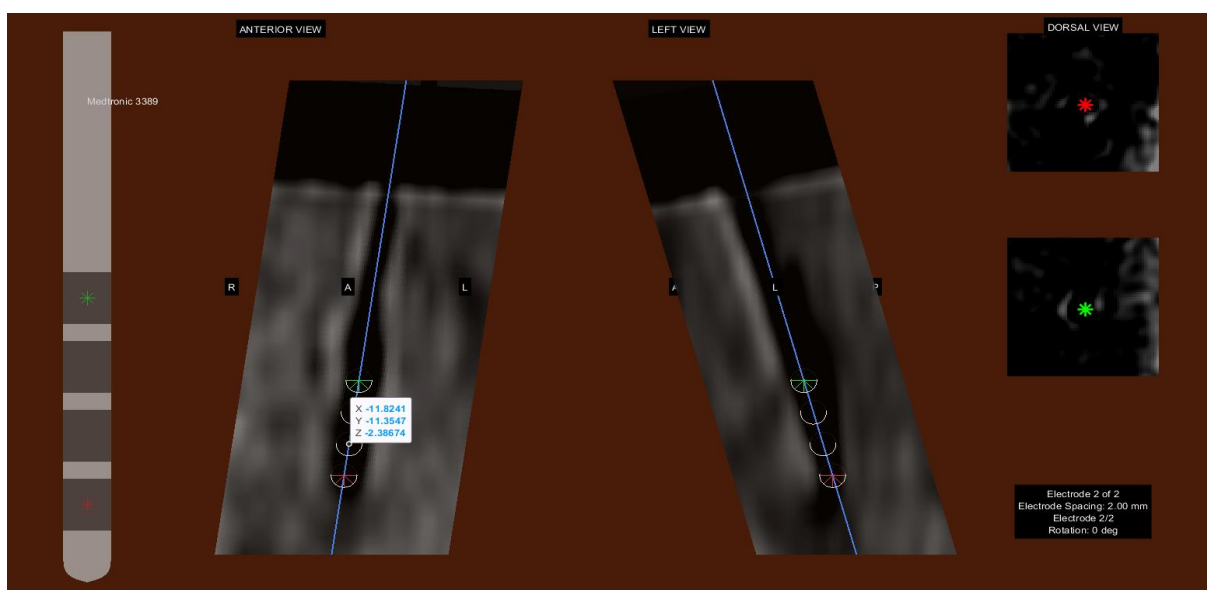
Figure 11: Manual electrode placement of left-side electrode. NH coordinates of selected contact. The electrode is identified by the artifact produced by the electrode in postoperative scan. The dorsal view (top right) shows the trajectory from above whereas the anterior and left view identify the downward trajectory.

The Table 3 below includes the coordinates of the selected contacts used for each patient. Some patients had additional coordinates provided. These coordinates identified a different contact that was in a closer proximity to the selected target point within the mSTN.

Table 3: Electrode contact coordinates. The table shows the X, Y and Z coordinates for each patient contact that was used in real time with additional coordinates provided if a closer point was identified.

Patient	Left	Right
VG	(8) X = -11.3147, Y = -13.0977, Z = -11.8304 (12,13,14) X = -13.0276, Y = -11.0453, Z = -8.7826	(0) X = 10.3440, Y = -13.9624, Y = -12.0806 (1,2,3) X = 10.4265, Y = -12.9343, Z = -10.2443 (7) X = 12.4462, Y = -11.2169, Z = -7.1772
GL	(12,13,14) X = -12.0751, Y = -12.0402, Z = -3.9583 (9,10,11) X = -11.5965, Y = -12.6993, Z = -5.7849	(5,6) X = 13.8109, Y = -12.9792, Z = -1.8783 (0) X = 13.1021, Y = -14.7352, Z = -5.4630
MB	(9,10,11) X = -13.6032, Y = -9.5461, Z = -5.5408	(0) X = 11.5926, Y = -12.6393, Z = -5.7234
AW	(9,10,11) X = -11.8620, Y = -5.1263, Z = -3.9137 (8) X = -10.7535, Y = -5.8721, Z = -5.5417	(1,2,3) X = 10.4150, Y = -6.2393, Z = -5.2281 (0) X = 10.3584, Y = -7.1261, Z = -7.1376
KN	(12,13,14) X = -11.4055, Y = -9.8699, Z = -3.8069 (8) X = -9.5952, Y = -12.1104, Z = -6.6597	(7) X = 12.9916, Y = -6.8656, Z = -6.1266 (0) X = 11.1534, Y = -10.3416, Z = -10.6585
MS	(8) X = -8.79448, Y = -16.3265, Z = -5.0534 (9,10,11) X = -10.1673, Y = -14.9804, Z = -4.1949	(0) X = 16.2993, Y = -10.4196, Z = -7.4880
TM	(0) X = -12.9334, Y = -12.1737, Z = -5.0464 (active)	(1) X = 11.3513, Y = -9.1454, Z = -7.2520 (active) (0) X = 10.4578, Y = -10.4611, Z = -8.4647
BD	(2) X = -10.5359, Y = -8.2810, Z = -4.1930 (active) (0) X = -9.4879, Y = -10.9025, Z = -7.0274	(2) X = 11.7485, Y = -7.8423, Z = -6.6590 (active) (0) X = 10.4546, Y = -10.2682, Z = -9.5643
GB	(1) X = -11.9141, Y = -18.0115, Z = -0.3535 (active) (0) X = -11.2887, Y = -18.2346, Z = -2.2401	(1)X = 13.5467, Y = -15.8465, Z = -1.9673 (active) (0) X = 12.8533, Y = -16.1929, Z = -3.81105

NH	(1) X = -11.8241, Y = -11.3547, Z = -2.3867 (active) (0) X = -11.3984, Y = -12.3116, Z = -4.0906	(2) X = 14.3180, Y = -12.8841, Z = -1.6719 (active) (0) X = 14.3180, Y = -12.8841, Z = -1.6719
JSc	(0) X = 16.2993, Y = -10.4196, Z = -7.4880	(2) X = 14.1854, Y = -9.97163, Z = -4.9822 (active) (0) X = 12.2732, Y = -12.0614, Z = -7.8065
GW	(0) X = -8.3178, Y = -8.3416, Z = 28.667 (active)	(0) X = 13.3546, Y = -6.1457, Z = 28.6426 (active)
BP	(1) X = 10.4922, Y = -19.5598, Z = 2.2891 (active) (0) X = 10.0360, Y = -20.0484, Z = 0.5679	(1) X = 10.4922, Y = -19.5598, Z = 2.2891 (active) (0) X = 10.0360, Y = -20.0484, Z = 0.5679

3.3 Individual Patient Data

TM (appendix A) had voltage set at 1V on contact 1 on the right-side electrode. It was identified that this contact was 5.68mm from the selected target area within the motor region of the right-side STN. The electrode itself was successfully placed within the STN with the VTA (represented by a red electrical field known as an e-field) firmly active with the motor and associative areas of STN. Contact 0 was approximately 10% closer to the STN target point and would allow for a reduction from 1V to 0.9V. Contact 0 on the left side electrode, currently selected was the optimum position. The electrode was placed outside of the left STN also in close proximity to the red nucleus (RN) however, no modifications were required as contact 0 was closest to the left STN target point with a distance of 3.06mm. The VTA on the left electrode made contact with the side of the motor area of the STN.

BD (appendix B) had a voltage set at 2.4V onto contact 2 with a distance of 6.83mm from right STN target point. The electrode was in close proximity to the side structures: pre-frontal, temporal, pre-motor and sensorimotor regions of the GPi, the VTA was activating the central portion of STN with stimulation on motor and associative areas. Contact 0 was deemed to be the optimum electrode with a distance of 5.66mm from target point. A 17% reduction in distance identifies a potential stimulus reduction to 2V. The left side electrode VTA was also in a close proximity to the side structures of the left side GPi, whilst stimulating a large central portion of the STN. A distance of 7.33mm was observed. The suggested optimum contact was 0 opposed to contact 2 at a distance of 5.17mm. This would allow for a 30% reduction 3V to 2.1V.

GB (appendix C) had a voltage set at 1.3V on contact 1 of the right electrode. The electrode was inserted in a deeper position and did not pass through the right STN; however, the smaller voltage

suggests a specific target area in the STN had been activated as the VTA was only slightly protruding the motor area of STN. Contact 1 was 5.22mm from target coordinates. Contact 0 was suggested as the optimum electrode with a distance of 3.62mm. This identified a 30% reduction in distance and theoretically would allow for 0.9V to be placed opposed to 1.3V currently used. The left side electrode was placed centrally into the left STN predominantly in the associative area of STN. The current contact 1 was 7.62mm to target point. Contact 0 was 16% closer and would allow for a reduction to 1.5V from 1.8V. The VTA encompassed most of the motor region of the left STN.

NH (appendix D) had voltage set at 1.5V onto contact 2 (figure 10) of the right electrode. The distance measured to the target point within the STN was 5.69mm. Contact 0 was identified to be a distance of 2.32mm, 59% closer and would result in a reduction to 0.61V to theoretically produce same effect. The left electrode had 1.5V on contact 1. The distance measured was 5.75mm. Contact 0 was a distance of 4.06mm, 29% closer with a potential voltage to 1.1V. The VTA for both electrodes is located outside of each STN.

JSc (appendix E) had a stimulus of 1.5V on contact 2 of the right electrode at a distance of 5.07mm. Contact 0 was observed as 2.74mm from target point identifying a reduction of 46% resulting in a stimulation of 0.8V. The left electrode with a stimulation of 1.5V on contact 0 was identified to be in the optimum position with a distance of 0.57mm. The VTA from both electrodes were firmly located within each STN respectively.

GW (appendix F) provided inaccurate information, the electrodes both appeared to be in good positions with respect to each STN however, the coordinates produced a significantly higher distance in comparison to other electrode placements. The VTA from each electrode was also localised to each STN further identifying the inaccurate coordinates provided.

The final conventional electrode data set was BP (appendix G), 1.4V placed onto contact 1 of the right electrode produced a distance 10.90mm, the electrode was in close proximity to the RN. The optimum contact with respect to the target point was 0 with a distance of 10.03mm, a reduction of approximately 8% with a voltage adjustment to 1.3V. The VTA of the right electrode was identified to be outside of the STN. Contact 2 had been selected on the left electrode with a voltage of 1.4V at a distance of 13.33mm. The closest contact to the target point was 0 with a distance of 10.21mm, presenting a 23.4% reduction with a stimulation of 1.1V. The VTA was only slightly touching the left STN motor area. The increased distance of BP electrode placement when compared to other electrode placements is a result of the specific targeting of the DRT tract within the posterior subthalamic area (PSA), aiming to specifically alleviate tremor in patients and as such cannot be accurately compared with other patients that have specific STN targeting.

The first patient with multi-directional electrodes was VG (appendix H). On the right electrode 1mA was split 60% on contact 0 and 40% on contacts 1, 2 and 3. A distance of 5.85mm for 0 and 4.54mm for 1,2 and 3. The optimum contact was 7 with a distance of 3.38mm with a 25.5% reduction from the current closest used contact of 1,2,3. 1mA could be reduced to 0.7mA theoretically producing the same result. The VTA was observed on the underside of the STN. On the left electrode contact 8 was used with a stimulation of 0.7mA at a distance of 5.37mm. Contact 12,13 and 14 was approximately 27% closer with a distance of 3.90mm provided a potential reduction to 0.5mA with the same effect. Again, the VTA was very small only activating areas on the underside of the left STN.

GL (appendix I) had 3mA set on 2 of the 3 contacts in the second position on the right-hand STN namely 5 and 6 with a distance of 5.38mm. The electrode used was placed firmly within the Motor region of the STN with the VTA encompassing a large portion however, due to the contact used the distance had been increased to the target point. The suggested optimum electrode was contact 0 at a distance of 1.55mm allowing for a possible reduction to 0.9mA. Contacts 12,13 and 14 on the left electrode had a stimulus of 2.8mA. The VTA engulfed a large part of the central and dorsal lateral region of the left STN, however the activation sphere was close to the side structures of the left side GPi. The distance from contacts 12, 13 and 14 to target point was 4.07mm, contacts 9, 10 and 11 was 33.8% closer allowing for a reduction to 1.9mA. Interestingly, the left electrode which had a smaller stimulation in ring mode produced a larger Electrical field for VTA when compared to the right electrode that had only 2 from 3 electrodes active. Follow up data identified a reduction to 2.5mA (right) and 1.7mA (left) on the same contacts.

MB (appendix J) used contact 0 (right) and 9,10 &11 (left) with a stimulation of 1.5mA at 2.77mm (right) and 1mA at 5.19mm(left). Contacts used on each electrode were in the optimum position. The VTA from the right electrode was firmly located within the STN close to the motor area. The left electrode was located outside of STN as was the VTA however, both electrodes sufficiently alieviated symptoms with no follow up patient data available.

The data from JS provided coordinate data however, an issue remained identifying the VTA, as a result information from JS could not be used.

AW (appendix K) had 1mA onto contacts 1, 2 and 3 at a distance of 8.90mm, the VTA was located predominately with the limbic area of the STN. The suggested optimum electrode was contact 0 at a distance of 7.91mm allowing for an 11.2% reduction to 0.9mA. Contacts 9, 10 and 11 was located outside of left STN with a distance of 9.97mm to target point. The suggested optimum contact was 8 with a distance of 9.09mm, allowing for a reduction to 0.9mA. The VTA was completely located outside

of the STN. Follow up data identified electrode stimulation increased to 2.8mA on the same contacts used on each side.

KN (appendix L) had 3mA on contact 7, identifying a distance of 7.67mm. contact 0 was 5.91mm from target point, producing a 22.3% reduction in distance resulting in a theoretical stimulus of 2.3mA. The electrode was placed within the limbic area of STN with the VTA located on the top end of the structure also close to the right side GPi. The left electrode had 3.5mA on contacts 12, 13 and 14. The distance was 5.91mm. Contact 8 was observed as 4.33mm resulting in a 26.7% reduction from 3.5mA to 2.6mA. A small e-field was produced on the underside of the left STN.

MS (appendix M) had 1.5mA set onto contact 0, this was the optimum contact given the position of the electrode. The distance was 5.17mm. Right side VTA was predominantly situated outside of the STN. DTI analysis (figure 12) identified activation of neuronal tracts to the Thalamus and Hippocampus. Contact 8 on the left electrode had been selected with a stimulus of 1mA at a distance of 5.13mm from target point. The optimum contact identified was 9, 10 & 11 at a distance of 4.14mm. This contact allowed for a 19.2% reduction in stimulation to 0.8mA to theoretically produce the same results. DTI analysis of the left electrode identified the VTA e-field activating Thalamus neuronal tracts. MS electrode placement specifically targeted the DRT neuronal tract within the PSA.
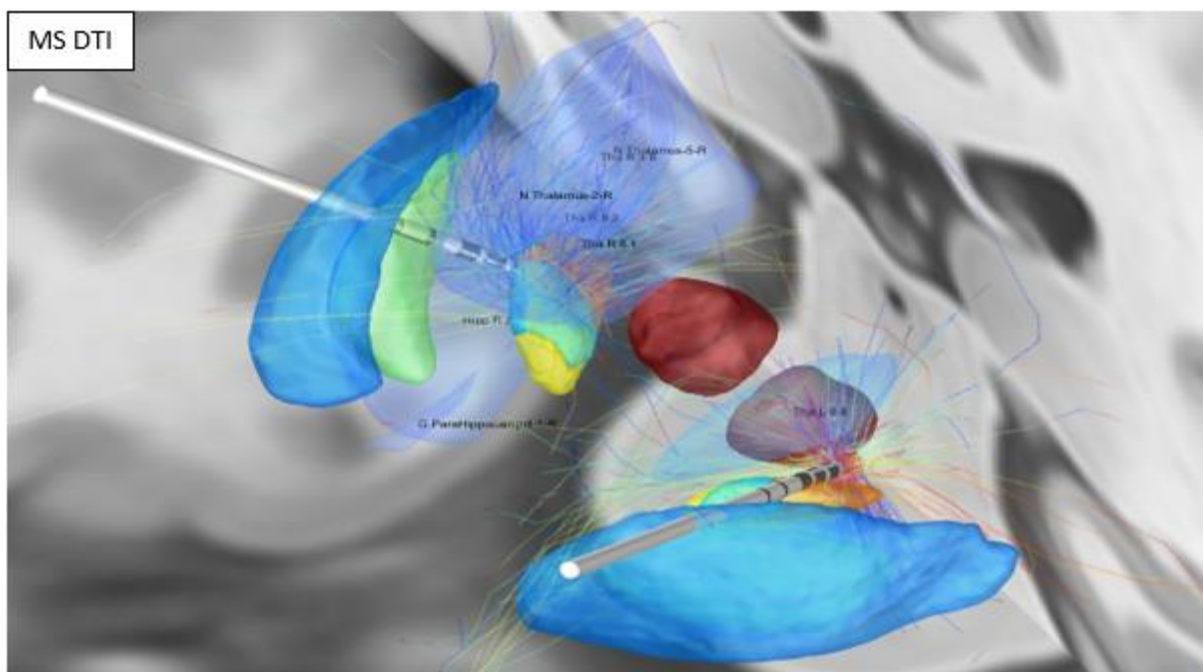
Figure 12: MS DTI image. PSA electrodes activating the Thalamus and Hippocampus (right) and the Thalamus (left) placement of electrodes targets the DRT tract to alleviate tremor symptoms in patients with PD.

JS was the only subject with multi-directional electrodes to be omitted from the final image of directional electrodes with all other electrodes successfully placed within close proximity to each STN. MS electrode placement targeted the PSA and shows a slightly different trajectory and was the only patient to undergo DTI analysis in Lead DBS. GW was omitted from the final Conventional electrode image as coordinate and image reproduction were inaccurate. BP electrode placement also targeted the DRTT in the PSA and can be seen as the only right-side electrode in close proximity to the RN.

The table below (Table 4) identifies the specific parameters for all patients. VG had a lower stimulation on the left electrode with the right electrode spilt. This was the only patient to have a stimulus split between two different contacts. The right electrode for GL was split however, this was on one contact. 13 patients from 14 had both their respective electrodes in ring mode with the only exception being GL with only one electrode in ring mode. The average distance in millimetres was approximately five. The closest electrode to the target point was JSc left with the furthest being both electrodes for BP. A trend was observed in patient stimulus. Voltage tended to be in a lower or higher range with only two electrodes (GL left & BD right) in the 2V range. A total of ten patients had a stimulus of 1.5V or lower with only three patients having either one or both electrodes at 3V or above.

Table 4: Patient electrode data. Each patient ID with corresponding stimulation of each electrode. (C) identifies the contact used. Ring mode identifies if directional contacts were used. Lastly, the distance of each selected contact to the selected coordinates within each STN. Patient JS results was not applicable as image reproduction and coordinates produced were incorrect, the same result was identified in patient GW.

Patient	Left voltage(V) (C)	Right voltage(V) (C)	Mode	Left distance(mm)	Right distance(mm)
VG	0.7(0)	1(0+1)(60%,40%)	Ring	5.37	5.85 & 4.54
GL	2.8(2)	3(2)	(L)Ring (R)13/14	4.07	5.38
MB	1(1)	1.5(0)	Ring	5.19	2.77
JS	1(2)	1(1)	Ring	N/A	N/A
AW	1(1)	1(1)	Ring	9.97	8.90
KN	3.5(2)	3(3)	Ring	5.91	7.67
MS	1(0)	1.5(0)	Ring	5.13	5.17
TM	1.2(0)	1(1)	Ring	3.06	5.68
BD	3(2)	2.4(2)	Ring	7.33	6.83
GB	1.8(1)	1.3(1)	Ring	7.62	5.22
NH	1.5(1)	1.5(2)	Ring	5.75	5.69
JSc	1.5(0)	1.5(2)	Ring	0.57	5.07
GW	1.3(0)	1.3(0)	Ring	N/A	N/A
BP	1.4(2)	1.4(1)	Ring	10.90	13.33

It was identified that a hypothetical reduction may be possible shown in table 5 if a closer electrode was identified in relation to the target point. From the 24 electrodes placed in twelve different

patients, it was identified that five electrodes were in the optimum location in relation to the selected location within each STN. A reduction can be observed in one or more electrodes in eleven of twelve patients with MS being the only patient to have both electrodes optimally placed. The largest reduction was observed from the right electrode of GL, which showed a significant drop from 3mA to 0.87mA. The left electrode of GL identified a reduction, all be it not as steep from 2.8mA to 1.9ma. A further three patients showed a similar trend namely KN (left and right), BD (right) and the right electrode of NH and JSc. A number of patients only required a small modification to stimuli including VG, AW, MS left, GB and BP.

Table 5: Patient electrode voltage data. Patient ID with active electrodes subject ID. JS and GW were omitted from the resulting data. The hypothetical closet electrode to the selected point within each STN and the corresponding potential reduction in stimulation if the closer electrode were to be implemented. Due to conditions in brain milliamps were directly proportional to Voltage.

ID	(L) active	(R) active	(L) closest	(R) closest	(L) reduction	(R) reduction
VG	8	0+1,2,3	12,13,14	7	0.7mA to 0.51mA	1mA to 0.7mA
GL	12,13,14	5,6	9,10,11	0	2.8mA to 1.9mA	3mA to 0.87mA
MB	9,10,11	0	Optimum	Optimum	n/a	n/a
AW	9,10,11	1,2,3	8	0	1mA to 0.91mA	1mA to 0.89mA
KN	12,13,14	7	8	0	3.5mA to 2.57mA	3mA to 2.31mA
MS	8	0	9,10,11	Optimum	1mA to 0.81mA	n/a
TM	0	1	Optimum	0	n/a	1v to 0.9v
BD	2	2	0	0	3v to 2.1v	2.4v to 2v
GB	1	1	0	0	1.8v to 1.5v	1.3v to 0.9v
NH	1	2	0	0	1.5v to 1.1v	1.5v to 0.61v
JSc	0	2	Optimum	0	n/a	1.5v to 0.8v
BP	2	1	0	0	1.4v to 1.07v	1.4v to 1.29v

3.4 Overall Patient Data Analysis

Volume of tissue activated was split into four broad sections (Figure 13), three of which formed part of the STN, namely the motor, associative and limbic. The area outside of the STN was also included. An overlap can clearly be observed, which identifies VTA crossing over the different sections.

Three of the electrodes, JSc (Left), MB (Right) and GL (Right) were solely placed in the motor region of the STN. The placement of each electrode was deemed to be in an optimum position as the mSTN is the main target to alleviate all round parkinsonian symptoms. The PSA located away from the STN towards the RN could also be considered to be an optimum position. However, this area would be a preferable target for patients that present with tremor as the dominant symptom.

There were five electrodes with VTA predominantly situated between the motor and associative region, this identified the main placement of electrodes in a more centralised position. A further two patients, each had one electrode in a central position with VTA crossing the border between the motor, associative and outside of the STN and one final patient who had VTA crossing between the mSTN and outside. In total, there were eleven electrodes from 26 situated in the mSTN that were reproduced in images (GW included). This was approximately 42% of all electrodes placed, with about 45% being CW electrode and 55% were MM electrodes.

The largest cohort of VTA was situated outside of the STN. It was noted that PSA electrodes specifically target neuronal tracts around the STN and therefore intentionally target areas external to the STN. There were 16 electrodes with VTA located outside of the STN, including overlap into the STN segments. This was approximately 62% of all electrodes VTA recorded.

Only one electrode, BD (Left) had VTA predominantly in the associative region. The VTA for AW (Right) was the only electrode to be activated solely in the limbic region of the STN, with KN (Right) VTA interacting between the limbic region and outside. The limbic region of the STN was not a desirable location as it is the furthest point within the STN to conventional target point of the motor segment.
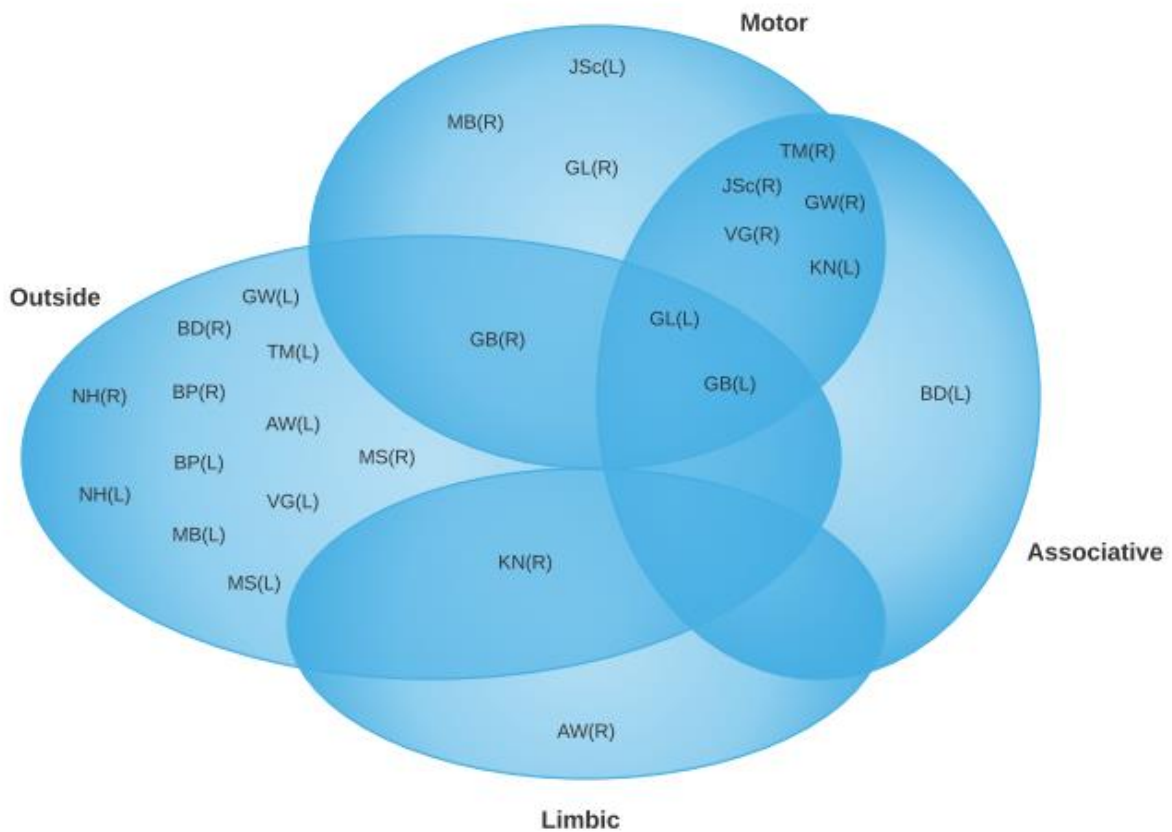
Figure 13: Volume of tissue activated in STN and surrounding area. The figure shows the association between the location of VTA from all viable electrode placements. The segments represent the three areas of the STN; motor, associative and limbic region. The fourth region selected was outside as this area could represent any electrode that was not placed inside the STN.

The corresponding electrode positions can be observed in figure 14 below. The complete image shows the overall electrode positioning for all MM and CW data sets that produced electrode coordinates. The image was constructed using lead group with the omission of the two non-viable data sets JS and GW. As seen in figure eleven, many of the electrode positions are located around the edge of each respective STN. The position may allow for activation of various neuronal tracts that are in close proximity.
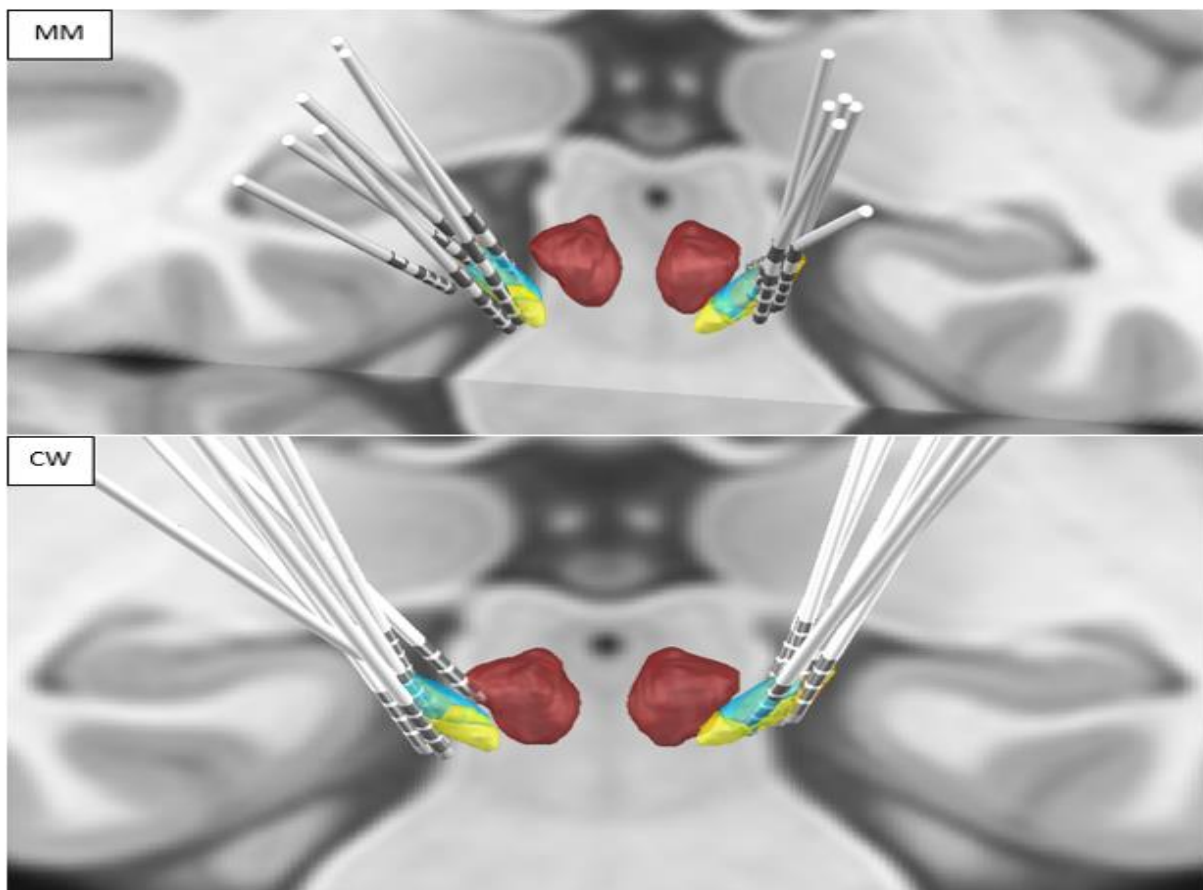
Figure 14: Complete image of electrodes. Complete image of final electrodes positions for all Multi-directional and Conventional electrode patients. The image shows the STN split into three sections, the motor region (orange), associative (blue) and limbic (yellow) region. The left and right RN can be observed (see appendices for image structure description).

4. Discussion

The need for new and improved methods to aid in the diagnosis and treatment of PD is essential as one hundred and forty people from every one-hundred thousand have developed PD (Tan et al., 2019). It is documented that patients with PD can suffer secondary mental health issues such as anxiety or depression and have an increased chance of developing dementia. A number of PD patients in an advanced stage of the disease will undergo DBS electrode placement surgery, with the purpose of ameliorating symptoms via an artificial electrical stimulus from an implantable pulse generator surgically placed into the body. DBS surgery is predominantly a later stage treatment when drugs such as levodopa have become less effective and potentially produced side effects including levodopa induced dyskinesia. In the case or young onset PD, surgical intervention may be utilised earlier as PD in younger patients tends to be more aggressive with dyskinesia becoming more prevalent in a shorter time frame.

4.1 Ameliorating Symptoms

A significant number of patients initially respond well to treatment however, overtime medication becomes less effective. It could be argued this same phenomenon can be observed in patients that are currently undergoing DBS. It was observed in 57% of cases that the stimulation required to mediate symptoms of PD had to be increased to produce the same results from the first programming session. This suggested that current treatments will only ameliorate symptoms for a limited time with patient outcome running parallel to disease progression. The main driving factor may be the volume of neuro degradation within the sub structures of the basal ganglia.

4.2 Electrode Placement

The first patient with conventional Medtronic 3389 electrodes was TM. In this patient, the right electrode was placed centrally between the motor and associative STN, with the left electrode making contact in the PSA area. Both electrodes were in a good position further validated with the lower voltage initially placed upon them. There were five other patient datasets that were placed in a more centralised location within the STN namely GB, JSc, GW, VG and MB. Of these, the right electrode of GB, both electrodes of JSc, GW, VG and MB all had lower voltages of 1.5V or lower. The lower stimulus, in combination with electrodes placed between the border of the motor and associative STN suggested that there may be a potential target point in that location. However, this could not be validated as each patient would need individual analysis on a case-by-case basis to confirm hypothesis.

The left electrode of BD was placed centrally more toward the limbic STN border similar to GB left, however, both electrodes were higher voltages of 3V and 1.8V respectively for the latter. The right electrode of both patients was located centrally but exterior to the STN in similar positions. Interestingly, there was a large disparity between the stimuli selected to ameliorate symptoms, namely 1.3V for GB and 2.4V for BD. This reiterated the individual level of disease progression identifying no solid correlation between location and stimulation as levels of neuronal degeneration varied from patient to patient.

The electrodes for NH were placed outside of each STN toward the RN, in the PSA. Of note, the VTA for both electrodes were firmly outside of the STN, which highlighted specific targeting of DRT tract, a common target for patients that present with tremor dominance to alleviate symptoms. BP had both electrodes placed in a similar position, again targeting the DRT tract in the PSA, similarly with a lower voltage of 1.4V for each electrode. The right electrode was protruding the RN, which was notable as the VTA was firmly apart from the red nucleus and with no observable side effects. This signified that both the electrodes were well placed and that the programming was correct. DBS of the RN is infrequently used, with studies conducted to alleviate oculopalatal tremor, but to no avail (Wang, et al., 2009).

Both electrodes used for JSc were centrally placed with a low voltage of 1.5V. The right electrode however was in a deeper position, and it was hypothesized that this may cause ocular problems given the deeper emplacement of the electrode close to the Field of Forel. It is suggested that the software placed the electrode in a slightly deeper position when compared to real time positioning. Alternatively, the right side STN for the patient was in a slightly different position, when using the standard template implemented by Lead DBS when rendering images 3D.

The electrode positioning for GW was well placed with the right electrode located centrally within the STN and the left electrode placed within the PSA, both of which had a low stimulation of 1.3V. Yet, the final image placement could not be used as coordinates gathered from the manual electrode placement step were significantly larger when compared to other data sets. The Z coordinates measured were positive 28.6 for both left and right. Additionally, the Z coordinates for JS were in an expected range however, no image was reproducible. Both data sets were inconclusive and therefore omitted. The observable coordinates for the Z axis were expected to be in the range of negative ten to positive ten.

Both electrodes for VG, the first patient with multi-directional electrodes were placed in a central position with regards to each STN. The right electrode had active contacts positioned lower when compared to other centrally placed electrodes such as JSc and TM.

GL produced interesting results, as the right electrode used two from three contacts on the second band (13, 14) at 3V with band two (12, 13, 14) of the left electrode placed in ring mode using 2.8V. Still, the VTA e-field for the right electrode was significantly smaller when compared to the left electrode. This anomaly was observed on different systems that had access to the patient data.

The e-field produced from both the right and left electrodes for MB was significantly small, given the stimulation was 1.5 (right) and 1 (left) mA, it is suggested that stimulation was split in 33% segments. However, this was enough to alleviate patient symptoms. Similar VTA e-field sizes were also observed with AW. Interestingly, the right electrode of AW was placed firmly in the limbic region of the STN a fair distance away from the normal target motor region, however the stimulation was enough to alleviate patient symptoms. It would have been expected a larger stimulus would be required, however, this was not the case. The left electrode was placed outside the STN but again required a lower stimulus suggesting the activation of an associated neuronal tract. Another interesting observation was between the right electrodes of MB and MS, in which each had 1.5mA placed on contact 0. However, as previously noted, the e-field of MB was significantly smaller, especially when compared to that of MS.

The left electrode of KN was placed in a central position within the STN predominantly within the associative region, requiring a larger stimulus of 3.5mA from the first programming session, this was in line with other electrodes placed in similar positions, namely BD left which was a similar stimulus. The left electrode was also placed toward the associative region, with a higher stimulus as expected.

4.3 Electrode Characteristics

The Medtronic 3389 and derivates thereof have been used with great success for a substantial period of time. The need for novel and improved methods to target structures more accurately has become ever more present given the advances in technology, the future direction of scientific innovation, the way PD progresses and our understanding of the disease. Simply asking the question of which electrode is better is far more complex, requiring a deeper more layered analysis to address the question.

The first aspect to consider is the level of difficulty to place the two sets of electrodes in the cranium of PD patients. There is minimal difference in this area with both electrodes taking the same approximate amount of time to place with the only variability being that of circumstances of the day of the procedure such as performing surgeon, staff present and image acquisition.

With regard to the safety and success of the electrodes, due to the advanced age of the Medtronic 3389 being approved by the FDA in September 1999, there is numerous data to confirm the safety of the electrode. A large study was conducted over an eight-year period in 38 different centres across Europe, North and south America with 2459 PD participants involved tracking the success of the implanted Medtronic DBS electrodes. The report stated lead events also known as lead survival had a survival rate of 89.9% over 14 years with a 95% probability (Medtronic, 2021). Boston Scientific vercise directional electrodes were released in January of 2019 (Boston Scientific, 2021.1) resulting in a significantly shorter time to conduct any long-term studies that follow patients throughout the course of their disease. The safety data for the multi-directional electrodes states no post-operative MR imaging should take place due to possible movement, damage to electrode and artifact development in produced images (Boston Scientific, 2021.2).

This raises the key point of the reliability of multi-directional images used for reconstruction in Lead DBS for the purposes of this study. The safety data from Boston Scientific states that artifact development may be an issue, resulting in all images of multi-directional electrode positions could be questioned (Boston Scientific, 2021.3).

It could be argued that the benefit of multi-directional electrode placement, although initially costly could prove cheaper over a longer period of time. The implementation and specific targeting by these electrodes may require less battery power from the IPG, resulting in fewer return visits including for surgical replacement of the IPG. This would benefit both the patient that does not require further surgery and the NHS as the surgical procedure does not need to take place.

The multi-directional electrodes did have a greater natural capacity when compared to conventional electrodes, given the directed capability of the first and second band and the lack thereof of the conventional electrodes. Taking into account the current direction of scientific innovation is it very feasible to assume in the coming years there will be significant advances in areas such as brain imaging and our understanding of PD generally. It may come to fruition that a specific target point, none of such identified in this study, or specific neuronal tract may be the optimal target location for PD to alleviate all symptoms and give patients a greater quality of life. In this instance, patients with multi-directional electrodes may have a significant advantage when compared to PD patients with conventional electrodes. The multi-directional ability of the electrodes may allow for a smaller VTA with a targeted approach; however, it could be argued that the time to reach that point will be years beyond the life expectancy of patients that had conventional electrodes initially installed.

4.4 DBS Optimization

Lead DBS, the computational software used for electrode placement visualization is a well-designed user-friendly interface which generates reproducible images in a short time frame. The software licence specifically prohibits the program as a diagnostic tool in a medical setting making the task of DBS optimization in a real world setting nearly impossible. The tool can be utilised for research purposes specifically to visualise VTA and potentially various neuronal tracts, on the provision there is an accompanying DTI data set to input into the software. The program attempts to cover all aspects with the aim of making the electrode positions as accurate of possible with options such as brain shift correction to accommodate electrode warping and electrode localisation, where the electrodes can be manually adjusted to fit in the artifact of post-operative images.

Rendered 3D images use several different atlases showing various substructures with the aim of targeting an area of interest directly. Firstly, images may be analysed in the Montreal neurological institute (MNI) space, a template of neuronal imaging that is an average of a set number of brain scans producing an approximation of the location of structures in the basal ganglia. A second approach is to use the patient native space; however, this method provides results that are unclear and ascetically unpleasing, and on many occasions the absence of key substructures. On numerous images, only the motor region of the STN was visible, with the associative and limbic notably absent. This raised issues with electrodes that may be placed external to the mSTN such as those of KN and AW. If there is no accompanying DTI data, then analysis may become particularly troublesome as electrodes appear to be in an unrelated location.

It may be possible to use the tool in several ways to improve the patient experience. Firstly, pre- and postoperative images from patients that are yet to have their first programming session could have their individual electrode placement analysed through Lead DBS to visualise final position. Different stimuli placed on all the contacts to visualise VTA may give an idea of what parameters may be best suited for the patient, in turn providing the neurologist a suggested set of data with the purpose of saving time and resources. This becomes especially relevant when using the multi-directional electrodes as there are a large number of combinations to check given there are eight contacts to choose from in different combinations including the positive contact that may be the case or any other contact that was not currently used. Secondly, the software may be used for quality assurance purposes checking that electrode positions are in close proximity to the defined target structure. It may highlight more advantageous trajectories and enhance surgical performance as imaging data can be viewed and improved upon where necessary.

4.5 Specific Target Point

For the purpose of this study a random point as close to the most central part of the motor STN was selected. It was deemed that none of the points within the STN reflected by the varying stimulation parameters were optimal. The most central point within each STN did not correlate with stimulation strength. JSc had the left electrode at 0.57mm with the right electrode at 5.07mm however, both had the same voltage placed upon them. One could draw a number of possible conclusions. Firstly, the selected coordinates that were placed within the most central part of the mSTN were not the optimum target, further identifying another point within the STN. Secondly, if the coordinates were correct then the level of degeneration would be different within each STN, which may be a possibility and would need to be assessed case by case with a visual assessment of each patient to identify if one side of their body is affected more so than the opposite side. It is more likely that another target point within the STN would be optimal. Based on our observations the dorsal lateral region of the STN was the optimum target structure. However, it could also be suggested that there may be more than one point within the mSTN that may be an ideal target. A number of patients had VTA located predominately above (NH, BP, GL & KN) and below (TM left, BD right, GB right, VG & MS) the STN following the initial programming session. Moreover, available data from follow up programming sessions identified NH and BP VTA were increased to touch the top section of the STN, with GL and KN VTA that was also located top side of STN decreased. Patients with VTA bottom side of STN also showed a similar pattern. TM left, and VG were increased, BD and GB right remained the same and no follow up data available for MS suggesting that VTA was sufficient. The two poles along the Y axis of the STN motor region suggest they may be good targets for electrode placement. This could be due to the activation of specific neuronal tracts exiting or entering these areas.

4.6 DTI

Only patient MS had DTI analysis, it was advantageous to observe the different neuronal tracts that had been activated as part of the VTA, namely tracts to the thalamus and the hippocampus. The thalamus is a key part of the direct and indirect pathway and receives equal stimulation producing an equilibrium like state that is observed in individuals that do not have movement and motor disorders. Activation of hippocampal neuronal tracts could be beneficial to the overall mental health of PD patients as studies done in rats identify electrical activation produce a BOLD response, (Scherf & Angenstein, 2017; Krautwald, Mahnke, & Angenstein, 2019) resulting in increased bloodflow to the area; however, further studies in humans would be required to establish this link. It could be argued that there is a large cross over of the underlying mechanism in the most common neurological diseases

such as AD and PD, one such link is the atrophy of the hippocampus, predominantly observed in AD. Moreover, a link has been established between hippocampal atrophy and non-motor symptoms in PD (Camicioli, et al., 2003). Patients that present with additional symptoms such as memory impairment, fatigue, anosmia and generalised cognitive decline may experience deficiencies in the hippocampus, possibly due to the effect of dopamine and the lack thereof received indirectly from SN (Calabresi et al., 2013). Observing the activation of different neuronal tracts, it may be suggested that PD patients who experience significant non-motor and movement problems in similar amounts could potentially have a second electrode placed between the STN and GPe with the purpose of stimulating hippocampal neuronal tracts as well as traditional STN associated pathways, however, at this point it is only theoretical.

DTI may become an important adjunct in the future of neurological imaging as it provides a greater picture of neuronal tracts in the human brain possibly allowing for a deeper individual analysis (Salama, et al., 2018). There are some drawbacks including the equipment required by hospitals to conduct DTI analysis. The standard MRI machines used by many hospitals have a magnetic strength of 1.5 tesla (T), which in itself is extremely powerful. Yet, the gold standard for DTI is a 3T MRI machine, which is twice the strength and extremely expensive and given financial constraints already in place within the NHS, it becomes difficult to justify if only for the sole purposes of PD imaging. The second drawback is the strength itself and the effects that may have on electrical equipment placed within PD patients. There are questions concerning the use of MM electrodes and postoperative imaging. The significant additional power provided from 3T MRI machines generate more heat and pose risks of overloading sensitive electrical equipment placed inside the body such as DBS electrodes potentially having a severe negative impact.

4.7 Limitations

There is no question that Lead DBS is an innovative software platform. There are several limitations and issues that arise from its use. There will always be uncertainty regarding the accuracy of the electrode placement when compared to real world electrode placement. Given the use of a template average of the basal ganglia leads to the conclusion that the electrode position may be in a different location from the actual position. This distance may be millimetres but the difference to patient outcome could be vast as the STN is small is size and would require a different stimulation strength to the possible parameters suggested.

A hallmark of PD is the development of protein aggregates especially in advanced stages and as surgery is normally reserved as a later stage treatment leads onto the possibility that obstructions

such as Lewy bodies or movement of electrode placement in real time may not be accounted for. Another variability of electrode placement was air that may have inadvertently entered the surface of the brain form the burr hole. The Lead DBS option to negate this was brain shift correction however, this extension proved troublesome to invoke as a number of error codes were produced on each attempt.

Observable issues with electrode reconstruction included the use of postoperative T2 images to place electrodes, the T2 image was a segment not a whole brain image, this proved difficult when compared to the use of postoperative T1 images. On many occasions, the automatic electrode placement did not work, resulting in manual placement of electrodes leading onto the possibility of human error. In order to correctly place electrodes, the contrast needed to be adjusted to observe the MRI artefact. However, this is essentially an estimate of how correct the electrode position looks. Some image artifacts were warped again suggesting some natural electrode movement during surgical placement. Of note, upon electrode visualisation all electrodes where completely straight leading onto the possibility of electrode contacts possibly being angled at a different trajectory.

On the second and third band of the Boston scientific electrodes contacts were split into three separate contacts. This raised the question of what contact is directly facing the point of interest. This was not so much an issue when placed in ring mode, however one patient (GL, right) had 2 from 3 contacts used, which does raise the question of the orientation of the electrode and is dependent of the software taking this into account. There are options to rotate the electrode, but without having in-depth knowledge of the surgical placement and follow up data, the trajectory of electrode contact is essentially an approximation, this may be an issue for electrodes that are not placed in ring mode as the activated contact could be facing a different direction rendering stimulation reconstruction inaccurate. Another limitation that arises was the use of voltage and amperes. All Medtronic electrodes used voltage as the selected stimulation parameter. Boston scientific electrodes are capable of having stimulation strength adjusted in amperes and volts. In the brain voltage and amperes are in a one-to-one ratio due to resistance, meaning one volt will equal one ampere. When more than one contact is available such as bands 2 and 3 on the multi-directional electrodes, an option is available to split the contacts into 33% divisions to make one. Alternatively, one volt or ampere can be set on each contact on a band resulting in the stimulation being trebled to three volts/amperes opposed to one volt/ampere that has been split into 33% segments. Data accumulated did not specify which option, so the latter was assumed again potentially providing a different result when compared to real time data.

Lastly, the use of UPDRS score would have been a good tool to quantify the levels of success of the surgery for each patient. There was no access to the data due to restrictions that were in place. This negated away from a good data point that may have shown a deeper understanding of surgical success however, for the purpose of this study it was not essential when comparing electrode characteristics and visualisation in Lead DBS.

4.8 Future Directions

There are different avenues which the research may be taken to build on the current study. The use of UPDRS score in this study would have been a very good indicator on how successful surgery could be and would provide another data point. This data could be coupled with electrode impedance and frequency to better analyse the electrodes and patient outcome in a larger cohort.

A good data point to implement would be DTI analysis of each patient. If individual neuronal tracts could be analysed, it might give insight into the possible hypothetical optimum parameters that may best suite individual patients coupled with a greater understanding the different neuronal tracts activated. This data could be compared to other patients that may have electrodes in a very similar position and the observable changes in neuronal tracts may be analysed as a level of neuronal degeneration may be observed in specific areas such as the basal ganglia.

A study following a set number of patients who undergo regular MRI scanning at set intervals though out disease progression may give insight into the changes of VTA. Although VTA is not a disease progression marker it may show that due to levels of neuronal degeneration VTA is increased to ameliorate symptoms. The aim could be to quantify neuronal degeneration. The study could potentially be validated or disproved by comparing the hypothetical electrode placement with real time placement to determine the accuracy of the Lead DBS software.

Lastly, the potential use of Lead DBS to determine the optimum contact and stimulation to be placed, providing the relevant information to the neurologist with the purpose of identifying if there is any correlation between suggested contact and actual contact used.

4.9 Conclusion

To conclude, twelve from 14 electrodes were successfully placed using Lead DBS. Coordinates were gathered and the distance was successfully measured from the target point to the activate contact currently in use. A hypothetical stimuli correction was used to accommodate the decrease in distance

if a closer electrode was identified. One patient had DTI analysis that identified VTA of neuronal tracts to the thalamus and hippocampus. Overall, the study was successful in reproducing an image from the pre- and post-operative data initially collected. Further research would be required to optimize DBS, as there are specific aspects that may not be currently transferable such as the use of MM electrodes postoperatively.

1) Which type of electrode is more effective to ameliorate symptoms?

It was not possible to determine which type of electrode would be more successful in ameliorating symptoms given the small patient cohort and lack of UPDRS3 scores to observe patient outcome.

2) Can DTI tractography be used to lower volume of tissue activated outside of desired area and potentially identify activated neuronal tracts?

It was not possible to determine if DTI could be used to lower volume of activated outside of desired area as only one patient had DTI data available. Data available could be placed into Lead DBS to observe what neuronal tracts may be hypothetically activated, but from a clinical standpoint this data would not be relevant at this stage.

3) Is the new multi-directional electrode approach quicker and easier than the widely used conventional method?

From a surgical standpoint, no one method is quicker as the process of placing the electrodes is very similar. The only difference possibly may come during programming sessions as the multi-directional electrodes have more contacts to test when compared to the Conventional electrodes; however, no data about the timing of programming session was recorded for the purpose of this study.

4) Can electrode stimulation be optimised?

Electrode stimulation could possibly be optimised but could not currently be done in Lead DBS as the software is for research purposes and not permitted in a clinical setting. Further research to compare hypothetical electrode positioning and real-world placement may indicate how accurate final electrode positions are potentially allowing for stimulation optimisation in a research setting.

5) Using Lead DBS, can a more specific point within the motor region of the subthalamic nucleus be identified as a target for DBS?

It is possible to identify a specific target point within the mSTN using Lead DBS, however the target may not be suitable in a clinical setting. An optimum location to target for DBS electrode placement could not be identified in this study.

5. References

Ahlskog, J., & Muenter, M. (2001). Frequency of levodopa-related dyskinesias and motor fluctuations as estimated from the cumulative literature. *Movement Disorders*, 16(3), 448-58.

Alves, G., Forsaa, E., Pedersen, K., Gjerstad, M. D., & Larsen, J. (2008, September). Epidemiology of Parkinson's disease. *Journal of Neurology volume, 255*, 18-32. doi:10.1007/s00415-008-5004-3.

Bezaed, E., Brotchie, J., & Gross, C. (2001). Pathophysiology of levodopa-induced dyskinesia: Potential for new therapies. Nature Reviews Neuroscience, 2(8), 577-588.

Betarbet, R., Sherer, T., & Greenamyre, J. (2005). Ubiquitin-proteasome system and Parkinson'sdiseases. Experimental Neurology, 17-27. doi: 10.1016/j.expneurol.2004.08.021.

Board, N. C. (2013, April). Clinical Commissioning: Deep Brain Stimulation (DBS) in Movement Disorders.

Boston Scientific. (2021, March 10). *https://news.bostonscientific.com*. Retrieved from news.bostonscientific.com: https://news.bostonscientific.com/2019-01-24-Boston-Scientific-Launches-Vercise-TM-Primary-Cell-And-Vercise-Gevia-TM-Deep-Brain-Stimulation-Systems-With-Directional-Leads#:~:text=Boston%20Scientific%20Launches%20Vercise%E2%84%A2,Directional%20Leads%20%2D%.

Boston Scientific. (2021, March 10). *MRI guidelines for Boston Scientific Deep Brain stimulation Systems.* Retrieved from https://www.bostonscientific.com/: https://www.bostonscientific.com/content/dam/Manuals/eu/current-rev-fr/91098813-02_RevC_ImageReady_MRI_Guidelines_for_Boston_Scientific_Deep_Brain_Stimulation_Systems_multi_OUS_S.pdf.

Boston Scientific. (2021, March 10). *Vercise DBS physicians manual.* Retrieved from www.bostonscientific.com: https://www.bostonscientific.com/content/dam/Manuals/us/current-rev-en/92093580-03_Vercise%E2%84%A2_DBS_Physician_Manual_s.pdf.

Brocks, D. (1999). Anticholinergic drugs used in Parkinson's disease: An overlooked class of drugs from a pharmacokinetic perspective. *Journal of Pharmacy & Pharmaceutical Sciences*,2(2), 39-46.

Cheng, H.-C., Ulane, C. Brooks, D. J. (2012). Parkinson's disease: Diagnosis. *Parkinsonism and Related Disorders*, 531-533. doi: 10.1016/S1353-8020(11)70012-8.

Calabresi, p., Picconi, B., Tozzi, A., Ghiglieri, V., & Filippo, M. D. (2014). Direct and indirect pathways of basal ganglia: a critical reappraisal. *Nature Neuroscience, 17*, 1022-1030.

Calabresi, P., Castrioto, A., Filippo, M., & Picconi, B. (2013). New experimental and clinical links between the hippocampus and the dopaminergic system in Parkinson's disease. *The Lancet Neurology*,12(8), 811-21.

Camicioli, R., Moore, M., kinney, A., Corbridge, E., Glassberg, K., & Kaye, J. (2003). Parkinson's disease is associated with hippocampal atrophy. *Movement Disorders* ,18(7), 784-90.

M., & Burke, R. E. (2010). Clinical Progression in Parkinson's Disease and the Neurobiology of Axons. *Annals of Neurology*, 67(6), 715-725.

Daubner, S., Le, T., & Wang, S. (2010). Tyrosine Hydroxylase and Regulation of Dopamine Synthesis. *Archives of Biochemistry and Biophysics*, 508(1), 1-12.

DeMaagd, G., & Phillip, A. (2015). Parkinson's Disease and Its Management. *Pharmacy & Therapeutics*, 40(8), 504-510.

Disease, M. D. (2003). The Unified Parkinson's Disease Rating Scale (UPDRS): Status and recommendations. *Movement Disorders*, 18(7), 738-50.

Eagle, D., Wong, J., Allan, M., Mar, A., Theobald, D., & Robbins, T. (2011). Contrasting roles for dopamine D1 and D2 receptor subtypes in the dorsomedial striatum but not the nucleus accumbens core during behavioral inhibition in the stop-signal task in rats. *The Journal of Neuroscience*, 31(20), 7349-56.

Eiyama, A., & Okamoto, K. (2015, April). PINK1/Parkin-mediated mitophagy in mammalian cells. *Current Opinion in Cell Biology, 33*, 95-101. doi: 10.1016/j.ceb.2015.01.002.

Finberg, J., & Rabey, J. (2016). Inhibitors of MAO-A and MAO-B in Psychiatry and Neurology. *Frontiers in Pharmacology*. doi: 10.3389/fphar.2016.00340.

Freeze, B., Kravitz, A., Hammack, N., Berke, J., & Kreitzer, A. (2013). Control of Basal Ganglia Output by Direct and Indirect Pathway Projection Neurons. *The Journal of Neuroscience*. 33(47), 18531-18539.

Gerlach, M., Double, K., Leblhuber, f., Tatschner, T., & Riederer, P. (2003). Dopamine receptor agonists in current clinical use: comparative dopamine receptor binding profiles defined in the human striatum. *Journal of Neural Transmission*, 110(10), 1119-27.

Gibb, W. (1992, May). Neuropathology of Parkinson's disease and related syndromes. *Neurological Clinics, 10*(2), 361-376.

Grinblat, Y., & Lipinski, R. (2019). A forebrain undivided: Unleashing model organisms to solve the mysteries of holoprosencephaly. *Developmental Dynamics*. doi.org/10.1002/dvdy.41.

Hospitals, N. T. (2017, June). Deep Brain Stimulation (DBS) Pre-operative information for People with Parkinson's Disease.

Jin, S., & Youle, R. (2012). PINK1- and Parkin-mediated mitophagy at a glance. *Journal of Cell Science*, 125(4), 795-799.

Kalogeropulou, A., Zhao, J., Bolliger, M., Memou, A., Narasimha, S., Molitor, T., . . . Nichols, R. (2018). P62/SQSTM1 is a novel leucine-rich repeat kinase 2 (LRRK2) substrate that enhances neuronal toxicity. *Biochemical Journal*, 475(7), 1271-93.

Klein, C., & Westenberger, A. (2012). Genetics of Parkinson's Disease. *Cold Spring Harbor Perspectives in Medicine*. 2(1), doi: 10.1101/cshperspect.a008888.

Krautwald, K., Mahnke, L., & Angenstein, F. (2019). Electrical Stimulation of the Lateral Entorhinal Cortex Causes a Frequency-Specific BOLD Response Pattern in the Rat Brain. *Frontiers in Neuroscience*. doi:10.3389/fnins.2019.00539.

Krishna, R., Ali, M., & Moustafa, A. (2014). Effects of combined MAO-B inhibitors and levodopa vs. monotherapy in Parkinson's disease. *Frontiers in aging Neuroscience.* Doi:10.3389/fnagi.2014.00180.

Lanciego, J., Luquin, N., & Obeso, J. (2012). Functional Neuroanatomy of the Basal Ganglia. *Cold Springs Harbor Perspectives in Medicine*. 2(12), doi: 10.1101/cshperspect.a009621.

Lau, L. D., Schipper, C., Hofman, A., Koudstaal, P., & Breteler, M. (2005, Aug). Prognosis of Parkinson Disease. *Arch Neurol, 62*(8), 1265-9.

Lu, F.-M., & Yuan, Z. (2015, June). PET/SPECT molecular imaging in clinical neuroscience: recent advances in the investigation of CNS diseases. *Quantitative Imaging in Medicine and Surgery, 5*(3), 433-447.

Lücking, C., Dürr, A., Bonifati, V., Vaughan, J., Michele, G. D., & Gasser, T. (2000, May 25). Association between Early-Onset Parkinson's Disease and Mutations in the Parkin Gene. *The New England Journal of Medicine, 342*(21), 1560-1567.

Maiti, P., Manna, J., & Dunbar, G. (2017). Current understanding of the molecular mechanisms in Parkinson's disease: Targets for potential treatments. *Translational Neurodegeneration*. doi: 10.1186/s40035-017-0099-z.

Masato, A., Plotegher, N., Boassa, D., & Bubacco, L. (2019). Impaired dopamine metabolism in Parkinson's disease pathogenesis. *Molecular Neurodegeneration*. 14(1), doi: 10.1186/s13024-019-0332-6.

Medtronic. (2021, March 10). *Medtronic 2017 Deep Brain Stimulation Systems.* Retrieved from https://asiapac.medtronic.com/content/dam/medtronic-com/products/product-performance/ppr-reports/2017-DBS-Report.pdf.

Merola, A., Zibetti, M., Artusi, C., Marchisio, A., Ricchi, V., & L Rizzi, e. a. (2012). Subthalamic nucleus deep brain stimulation outcome in young onset Parkinson's disease: a role for age at disease onset? *Journal of Neurology, Neurosurgery, and Psychiatry*, 83(3), 251-7.

Montgomery, M., Miner, N., Soileau, M., & McDonald, D. (2016). Placement of the AbbVie PEG-J tube for the treatment of Parkinson's disease in the interventional radiology suite. *Baylor University Medical Center Proceedings*, 29(4), 420-422.

Neve, K., Seamans, J., & Trantham-Davidson, H. (2004). Dopamine receptor signaling. *Journal of Receptor and Signal Transduction Research*, 24(3), 165-205.

Ovallath, S., & Sulthana, B. (2017). Levodopa: History and Therapeutic Applications. *Annals of Indian Academy of Neurology*, 20(3), 185-189.

Pandey, S., & Srivanitchapoom, P. (2017). Levodopa-induced Dyskinesia: Clinical Features, Pathophysiology, and Medical Management. *Annals of Indian Academy of Neurology, 20*(3), 190-198.

Park, K., Oeda, T., Kohsaka, M., Tomita, S., Umemura, A., & Sawada, H. (2018, Oct). Low body mass index and life prognosis in Parkinson's disease. *Parkinsonism & Related Disorders, 55*, 81-85.

Poewe, W., Antonini, A., Zijlmans, J., Burkhard, P., & Vingerhoets, F. (2010). Levodopa in the treatment of Parkinson's disease: an old drug still going strong. *Clinical Interventions in Aging*, 229-238, doi: 10.2147/cia.s6456.

Rand, M. K., Stelmach, G. E., & Bloedel, J. R. (2000, Feb). Movement accuracy constraints in Parkinson's disease patients. *Neuropsychologia, 38*(12), 203-212.

Redenšek, S., Trošt, M., & Dolžan, V. (2017). Genetic Determinants of Parkinson's Disease: Can They Help to Stratify the Patients Based on the Underlying Molecular Defect? *Frontiers in Aging Neuroscience*. doi: 10.3389/fnagi.2017.00020

Reichmann, H. (2017, October). Premotor Diagnosis of Parkinson's Disease. *Neuroscience Bulletin, 33*(5), 526-534.

Rinne, U., & Mölsä, P. (1979). Levodopa with benserazide or carbidopa in Parkinson disease. *Neurology*, 29(12), 1584-9.

Ross, G. W., Petrovitch, H., Abbott, R. D., Nelson, J., Markesbery, W., Davis, D., White, L. R. (2004). Parkinsonian signs and substantia nigra neuron density in decendents elders without PD. *Annals of Neurology*, 56(4), 532-9.

Rui, Q., Ni, H., Li, D., Gao, R., & Chen, G. (2018). The Role of LRRK2 in Neurodegeneration of Parkinson Disease. *Current Neuropharmacology*, 16(9), 1348-57.

Salama, G., Heier, L., Patel, P., Ramakrishna, R., Magge, R., & John, A. (2018). Diffusion Weighted/Tensor Imaging, Functional MRI and Perfusion Weighted Imaging in Glioblastoma—Foundations and Future. *Frontiers in Neurology*. doi: 10.3389/fneur.2017.00660.

Scherf, T., & Angenstein, F. (2017). Hippocampal CA3 activation alleviates fMRI-BOLD responses in the rat prefrontal cortex induced by electrical VTA stimulation. *Plos One*. DOI: 10.1371/journal.pone.0172926.

Solpsema, J., Pena, E., Patriat, R., Lehto, L., Grohn, O., Mangia, S., & al, e. (2018). Clinical deep brain stimulation strategies for orientation-selective pathway activation. *Journal of Neural Engineering*. 15(5), doi: 10.1088/1741-2552/aad978.

Qiu, M.-H., Yao, Q.-L., Vetrivelan, R., Chen, M., & Lu, J. (2016). Nigrostriatal Dopamine Acting on Globus Pallidus Regulates Sleep. *Cerebral Cortex*, 26(4), 1430-39.

Tan, M., Malek, N., Lawton, M., Hubbard, L., Pittman, A., Joseph, T., & Hehir, J. (2019). Genetic analysis of Mendelian mutations in a large UK population-based Parkinson's disease study. *Brain*, 142(9), 2828-44.

Thenganatt, M., & Louis, E. (2012). Distinguishing essential tremor from Parkinson's disease: bedside tests and laboratory evaluations. *Expert Review of Neurotherapeutics*, 12(6), 687-96.

Tieu, K. (2011). A Guide to Neurotoxic Animal Models of Parkinson's Disease. *Cold Spring Harbor Perspectives in Medicine*. 1(1), doi: 10.1101/cshperspect.a009316.

Tritsch, N., & Sabatini, B. (2012). Dopaminergic modulation of synaptic transmission in cortex and striatum. *Neuron*, 76(1), 33-50.

Tysnes, O.-B., & Storstein, A. (2017). Epidemiology of Parkinson's disease. *Journal of Neuro Transmission*, 124(8), 901-905.

Vaillancourt, D., & Newell, K. (2000, November). The dynamics of resting and postural tremor in Parkinson's disease. *Clinical Neurophysiology, 111*(11), 2046-2056.

Vasta, R., Nicoletti, A., Mostile, G., Dibilio, V., Sciacca, G., Contrafatto, D., & al, e. (2017). Side effects induced by the acute levodopa challenge in Parkinson's Disease and atypical parkinsonisms. *PLOS One*. 12(2), doi: 10.1371/journal.pone.0172145.

## 6. Appendices

Appendix A: Image TM
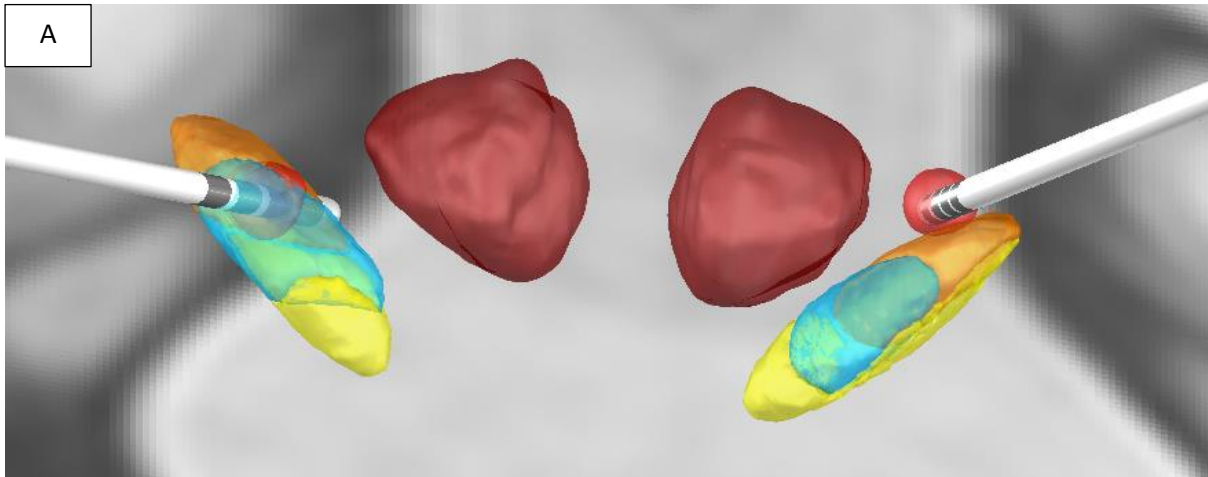
Appendix A shows the right electrode (place towards the left side) and the left electrode (towards the right side). The STN is split into three sections, orange is the motor STN, blue is associative, and yellow is the limbic area of the STN. The left and right red nucleus is present. The red sphere around each electrode contact point is the E-field produced by each electrode.

Appendix B: Image: BD
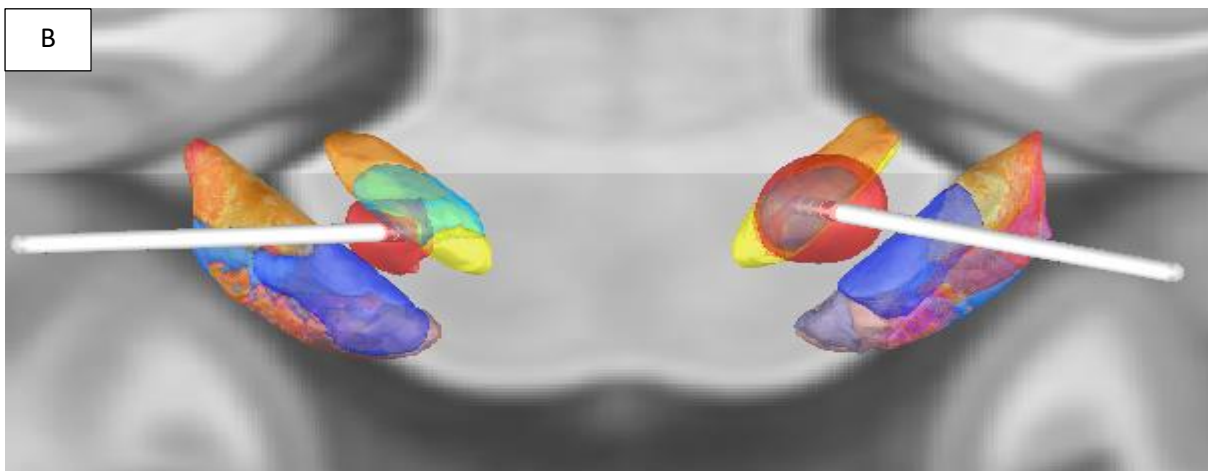
Appendix B shows the left and right STN with the same regions highlighted. Also present is the left and right GPi broken down into different sections. Purple is the GPi sensory, red is primary motor, green is premotor, orange is sensory motor, light blue is post-parietal, pink is occipital, maroon is temporal and dark blue is prefrontal.

Appendix C: Image: GB
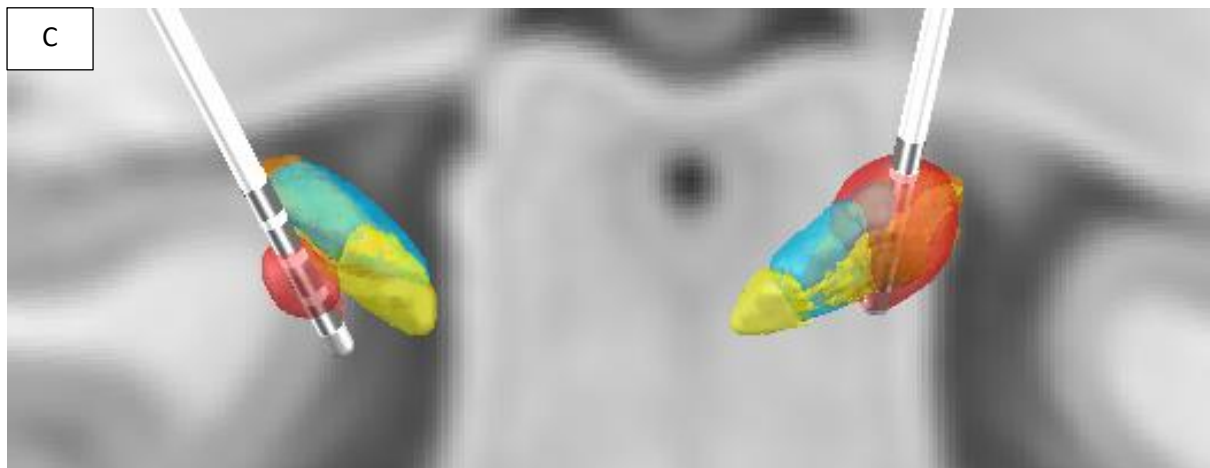
Appendix C shows the left and right STN dived into segments. The right-side electrode is positioned outside of the STN whereas the left electrode and corresponding E-field is located firmly inside the STN.

Appendix D: Image: NH
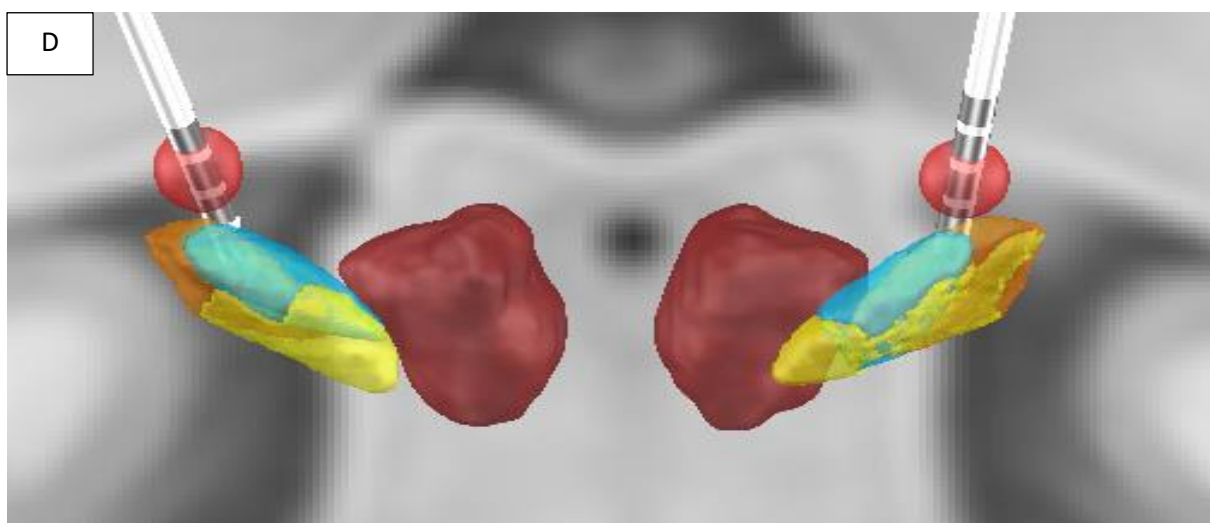
Appendix D shows the left and right STN and the left and right RN. Both electrodes are located outside of each STN, specifically targeting the PSA.
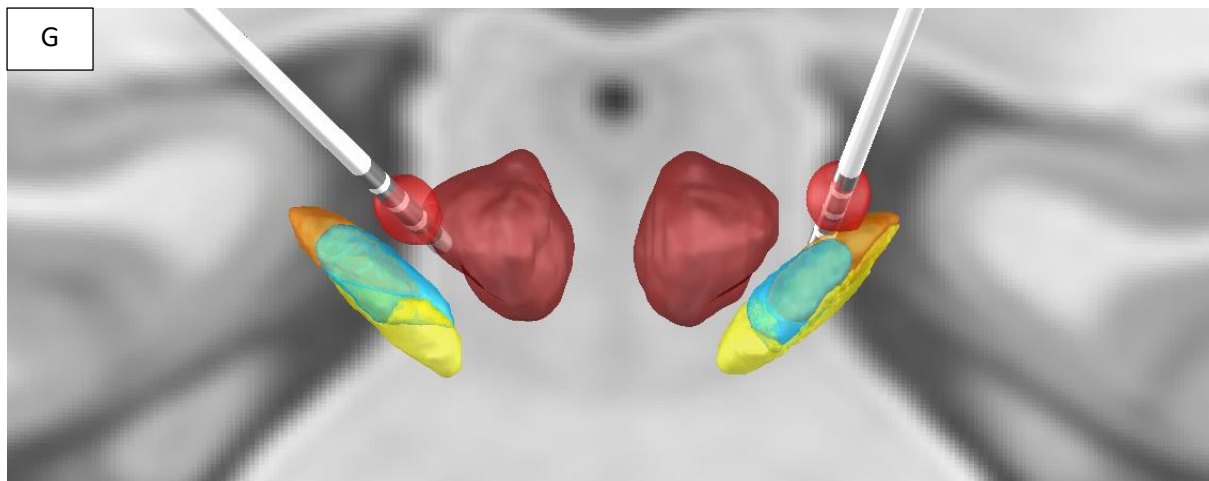
Appendix E: Image: JSc
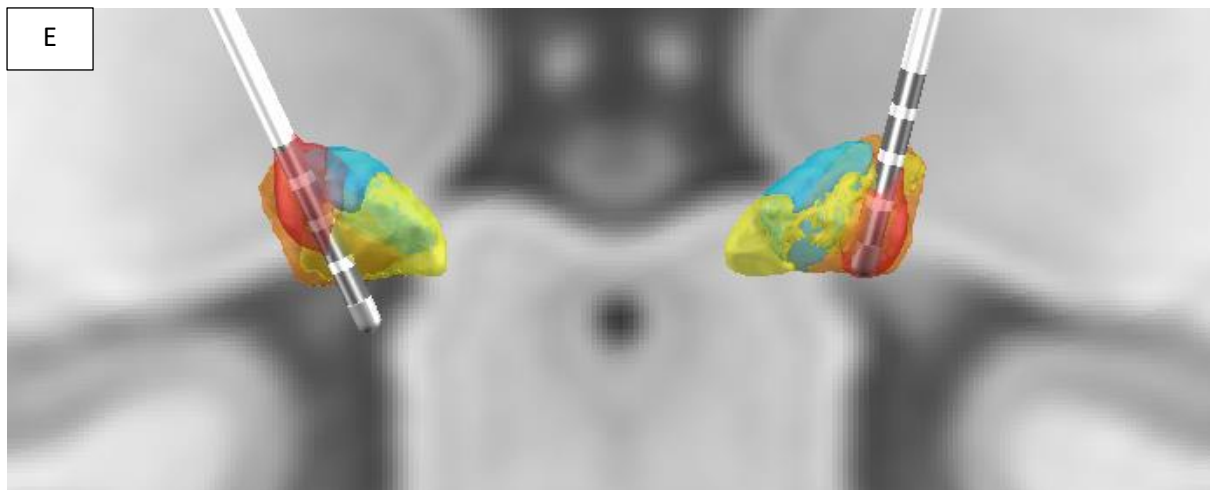
Appendix E show the left and right STN split into segments. The right electrode is in a deeper position with the left electrode located within the STN.

Appendix F: Image: GW
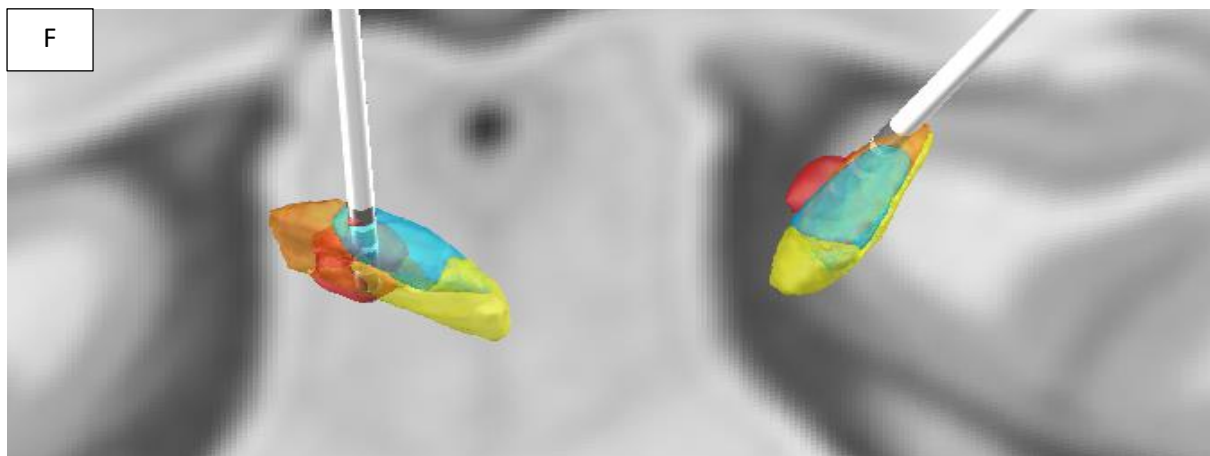
Appendix F shows the right electrode placed within the right side STN and the left electrode placed in the PSA.
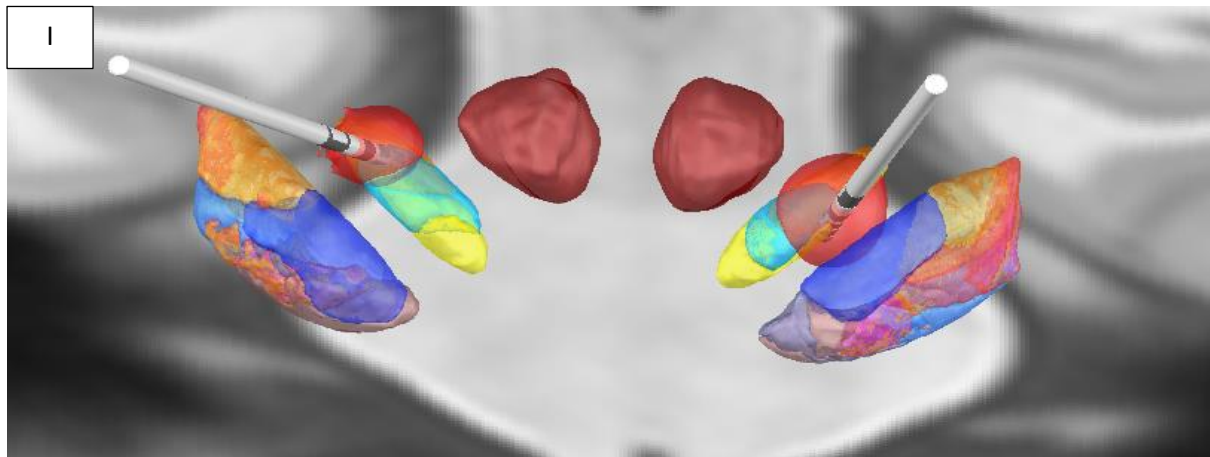
Appendix G: Image: BP

Appendix G shows each STN and RN with both electrodes located in the PSA

Appendix H: Image: VG
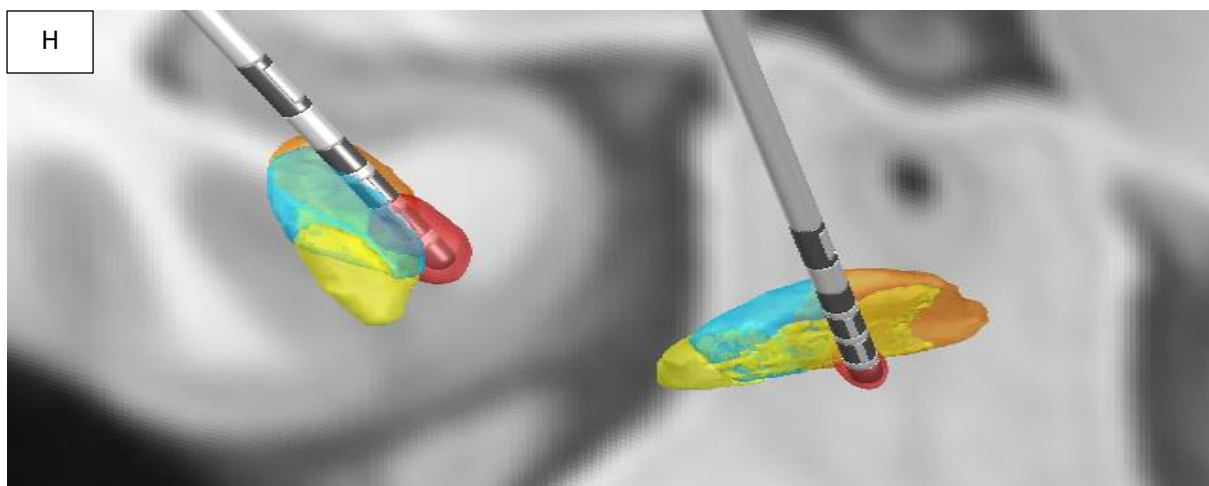
Appendix H shows the right electrode with VTA towards the underside of the right side STN and the left electrode VTA towards the underside of the left STN. The left VTA is also considerable smaller than the right side VTA.

Appendix I: Image: GL

Appendix I show the GPI, STN and RN on both sides. A large VTA is observable that engulfs each mSTN and also a portion outside of each STN respectively.

Appendix J: Image: MB
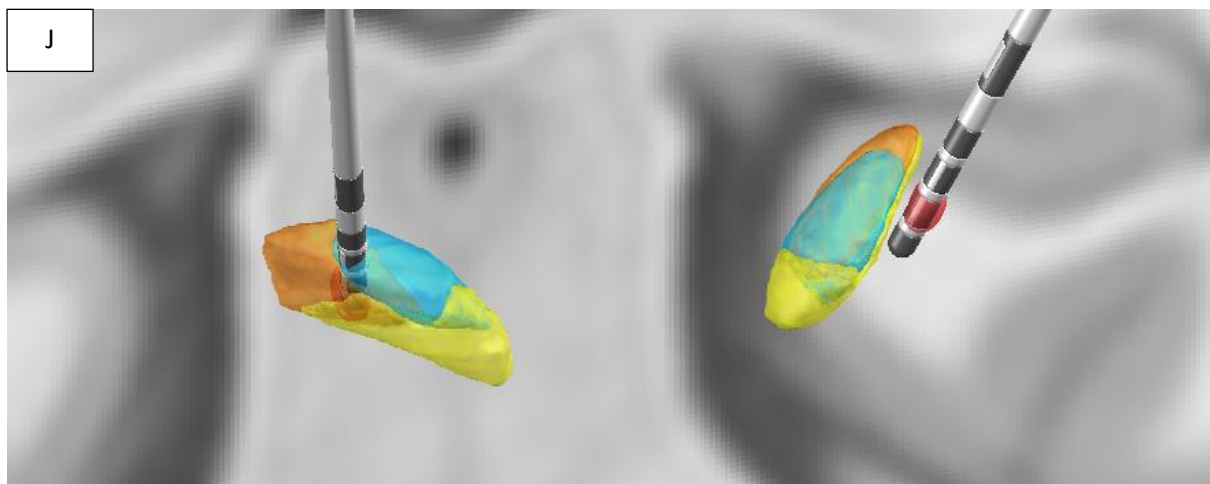
Appendix J shows the right electrode placed within the STN, the left electrode is placed away from the STN. The VTA e-field is notable small in each electrode respectively.
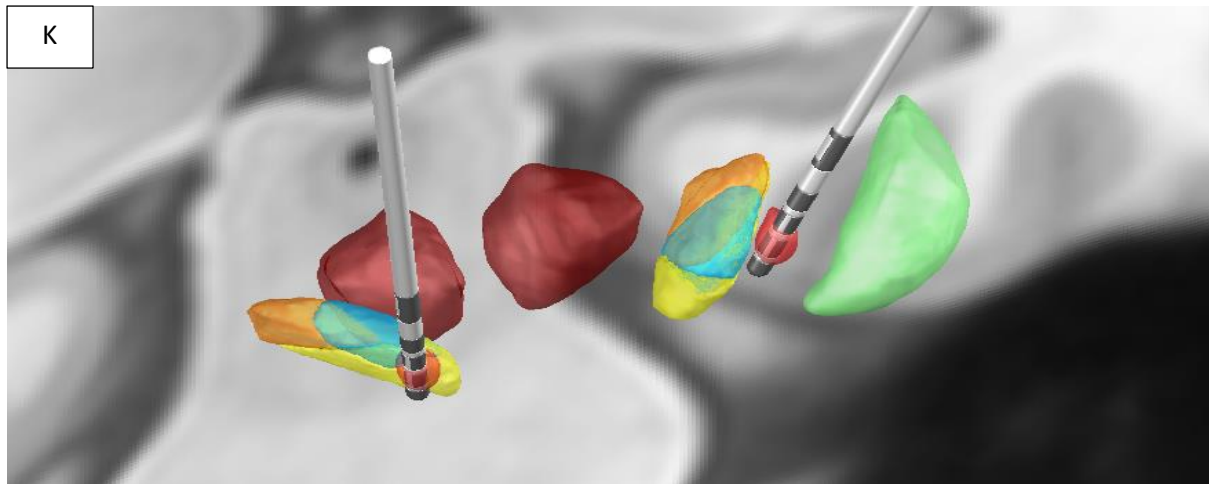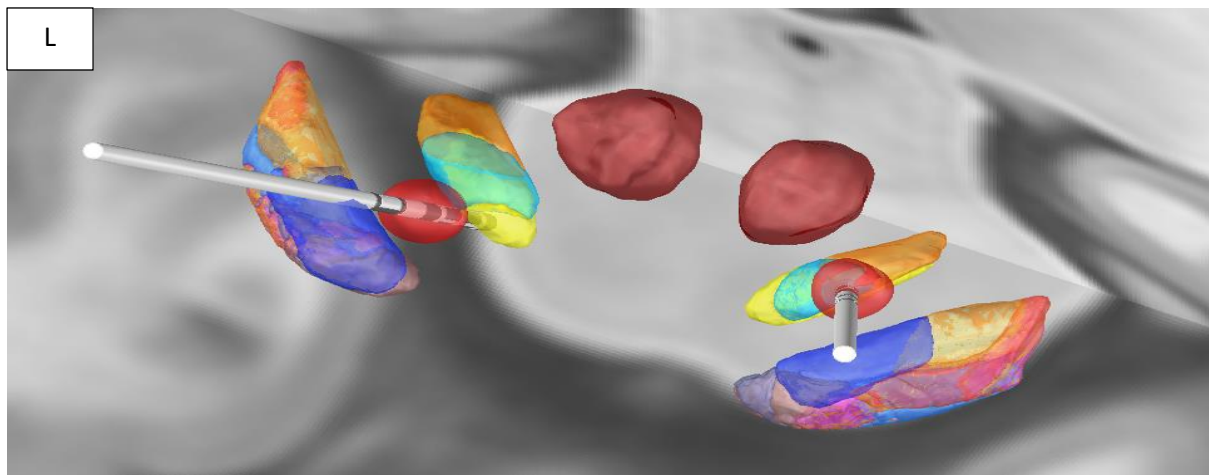
Appendix K: Image: AW

Image shows each STN and red nucleus. Also included is the left GPi, as a whole structure not broken down into sections.

Appendix L: Image: KN

Appendix L Shows the left and right GPI, STN and RN. The right electrode and corresponding VTA is located toward the limbic area of the STN. The left electrode and VTA and placed in a more centralised position.

Appendix M: Image: MS
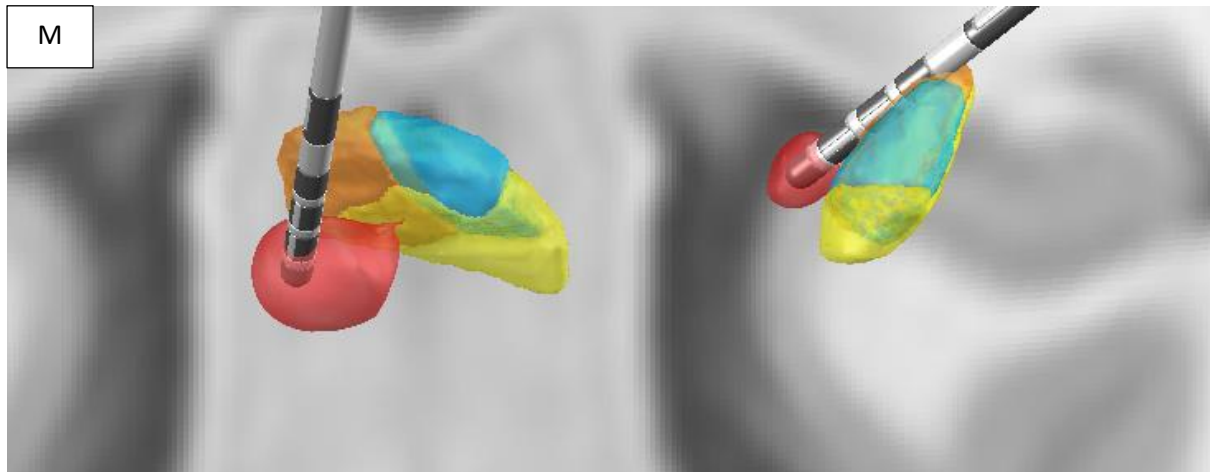
Appendix M shows the left and right STN. The right-side electrode is located outside the STN with a larger e-field when compared to the left e-field produced from the left electrode.